1514.

Off-chip Coupling

Wim Bogaerts – Diedrik Vermeulen

Ghent University – imec

Photonics Research Group

Contents

1 Introduction

The advantage of silicon photonics is its potential for large-scale integration. The key enabler there is the very high index contrast: as discussed in the previous chapter, light can be confined into a submicron waveguide core and guided in bends with radii of only a few micrometers. In addition, the potential of wafer-scale processing, integration of active components, electronics and even III-V semiconductors (topics discussed further in this book). However, the submicron waveguide core introduces a significant problem of its own: Coupling light into and out of the chip to the outside world. The standard for transporting light at telecom wavelengths is single-mode fiber where the optical mode has a mode-field diameter of 10.4µm at 1550nm and 9.2µm at 1310nm. This is illustrated in Figure 1. When joined together at the interface, coupling efficiency from one waveguide to the other is of the order of 0.1% (-30dB).

Bringing electrical signals off-chip is a relatively trivial challenge: a galvanic contact should be established, which can be done through wire-bonding schemes or flip-chip bumps. Electrical signals can be easily routed over various levels, materials and cross-sections. However, things become somewhat more complex when very high-speed signals need to be transferred: at that point careful RF design is required, and the effects of termination, impedance matching and crosstalk come into play. Similar constraints apply for photonics: light cannot just change direction, and when coupling between waveguides, one needs to take care of mode matching, reflections and crosstalk.

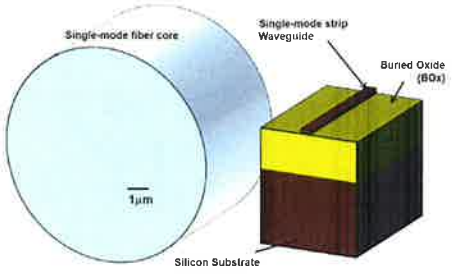

Figure 1: Optical mode size of a single-mode fiber and a silicon photonic wire waveguide, drawn to scale.

Therefore, efficiently converting light from a fiber into a submicron on-chip silicon waveguide and vice versa due to reciprocity, is a non-trivial challenge. This chapter will discuss the various approaches to address this problem.

The most common solutions for coupling are *in-plane* coupling, also often referred to as *edge* coupling, and *grating couplers*, which enable the coupling of light from the surface of the chip. These two solutions are schematically represented in Figure 2.

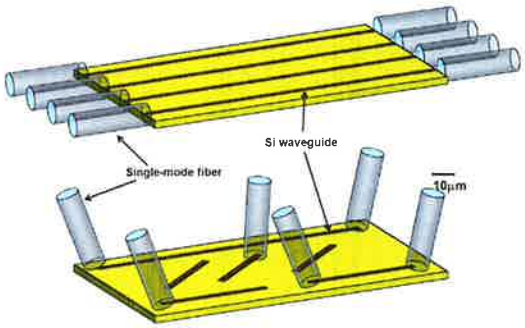

Figure 2: The two most common coupling solutions: (a) in-plane couplers, (b) out-of-plane couplers

In the next section, we will discuss some generic concepts relating to fiber-to-chip waveguide coupling, and introduce a number of metrics to evaluate the different solutions. In section 3 we focus on in-plane mode converters for edge-coupling solutions, while in section 4 we give a detailed overview of grating couplers for surface coupling. Section 5 steps away from fiber-based coupling solutions, looking at the options of coupling light from free space. In the conclusion in section 6, we recapitulate the different solutions and put them next to one another based on the criteria we defined in section 2.

2 Fiber-to-waveguide coupling

Before discussing the most common approaches of fiber-to-waveguide coupling, we will introduce some generic concepts which are common to all solutions. First of all, we will look at the generic problem of coupling between two waveguide modes, and discuss the mechanisms with which this can be efficiently accomplished. Based on that, we will look at the technical metrics which determine the efficacy of a specific coupling solution, so we can compare the different implementations on a somewhat objective basis.

2.1 Coupling mechanisms

If we consider the coupling between two single-mode optical waveguides, the modes in both waveguides should be matched both in real space and in k-space (impulse). Real-space matching means that the spatial distribution (i.e., the mode profile) of one waveguide should be converted into the mode profile of the other waveguide, such that the overlap integral is maximized [1]. If the modal overlap is not good, this will result in coupling to non-guided radiation modes, or if one of the waveguides is multi-mode, coupling to unwanted guided modes which can cause interference and mode-beating within the circuit.

Matching in k-space means that the difference in propagation vector between the guided modes of both waveguides is efficiently transformed by the coupler. This includes differences in magnitude and direction. This is the optical equivalent to impedance matching used in the microwave regime, and the effects of imperfect matching are similar: additional losses, scattering and especially back-reflection.

It is important to note that *coupling between optical modes* is bidirectional, unless strong nonlinear or nonreciprocal effects come into play, the coupling efficiency of a particular coupler in one direction is the same as in the other direction. In the case of single-mode waveguides, mode-to-mode coupling efficiency is equivalent to the overall power coupling efficiency. In the case of multimode waveguides, this is no longer the case, and there we should make a distinction between the power coupled to the desired guided mode and between excitation of unwanted higher order modes. Furthermore, if the vertical symmetry of the waveguide is broken, coupling between the different polarizations which are guided by the waveguide can occur.

We can discern several common mechanisms to handle both the spatial and impulse mismatch, and they have all been demonstrated to couple light from high-contrast on-chip waveguides to optical fibers. They are illustrated in Figure 3.

- **Adiabatic transition**: The simplest method to match the modes of two different waveguide cross sections is by a long adiabatic *taper* between the two waveguides. The length of the taper is mainly determined by the mismatch that has to be overcome and by the distance in k-space of the nearest modes which act as parasitic coupling channels. In the case of silicon photonic wires and single-mode fibers, this mismatch is quite large, and long taper sections are needed. Most edge-coupling solutions, discussed further in this chapter in section 3, are based on this principle.
- **Diffraction**: Periodic gratings scatter light at each grating tooth, and when all scattering contributions are in phase, constructive interference occurs. This effect can be used for coupling between two waveguides: By carefully tuning the scattering cross section and the period of the grating, the total scattered field can be tailored to match the target waveguide mode as close as possible. In addition, the periodicity of the grating has its own impulse, which transforms the impulse mismatch between the two waveguide modes. Because of this, the grating can also be used to change the direction of the light: for off-chip coupling, the light of the on-chip waveguide can be diverted out-of-plane. Such diffractive gratings or *grating couplers* are now the most commonly used technique for surface coupling to silicon photonic chips.
- **Multi-mode or multi-path interference**: A similar mechanism to diffractive coupling is multi-mode or multi-path coupling. In this approach, the light from the single-mode waveguide is distributed over multiple channels, which can be either different paths, or the modes of a multimode waveguide. By tuning the phase delays and magnitude of the different contributions, the resulting field at the entrance of the target waveguide

corresponds closely to the waveguide mode, enabling efficient coupling. A special case of this mechanism is *evanescent coupling*, as used in directional couplers. In that case, the light in two closely spaced waveguides is distributed over two supermodes (even and odd) and depending of the coupler length, a fraction of light is coupled from one waveguide to the other.

- **Resonant coupling**: A final approach is to couple both waveguides to a resonant structure. Here, the coupling should not necessarily be very high, as long as both coupling efficiencies are matched to the other loss mechanisms in the resonator. When properly designed and close to the resonance wavelength, the resonator will efficiently couple the light from the input to the output. Coupling between the resonator and the waveguides can be through various mechanisms, but most common is *evanescent coupling*.

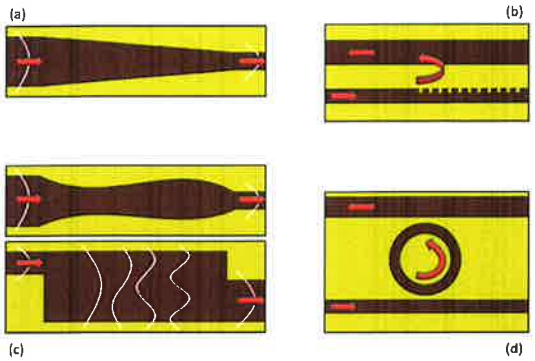

Figure 3: Coupling mechanisms: (a) adiabatic coupling, (b) diffractive coupling, (c) multi-mode coupling, (d) resonant coupling.

2.2 Coupling metrics

When looking at coupling solutions from a fiber to an on-chip waveguide, there are a number of metrics, apart from the coupled power, by which to evaluate the coupling efficiency.

- **Coupling efficiency**: For most applications, it is imperative to lose as little light as possible when making the transition from the fiber to the chip (and back). Power coupling efficiency, and its complement *insertion loss* (IL), are usually expressed in % or dB per interface. With coupling efficiency comes also the question of where the other fraction of the light is going. Couplers should have a low *back-reflection* into the fiber or on-chip waveguide, and non-coupled light should be channeled or absorbed to avoid *crosstalk*. We are generally interested in the optical power in a specific guided mode, so the coupling efficiency should always be calculated for the desired modes.
- **Polarization:** A single-mode fiber actually supports two guided modes with orthogonal polarization, which are usually degenerate. Because of that degeneracy, the actual polarization state in the fiber is unknown in many situations. From a chip point of view, the fiber polarization can be broken down in a transverse electric (TE) and a transverse magnetic (TM) component. The silicon waveguides can also support both polarizations, but unlike in the fiber, the optical properties of both polarizations are very different. Except for a few situations, it is important to have only a single polarization in the silicon waveguide. Still, from the fiber's point of view, the silicon circuit should function irrespective of the polarization in the fiber. Therefore, coupling both fiber polarizations correctly is an important requirement for a good coupling solution. A *polarization diversity* approach, which is discussed further in section 2.3, is an attractive solution to this problem. The most common metric to evaluate the polarization dependence is *polarization dependent loss* (PDL), which is expressed in dB, either per interface or for the entire chip.

- **Wavelength and Bandwidth:** Many potential applications require that the fiber-chip coupling solution has a broad coupling spectrum. The coupler should be able to handle the wavelength components in this spectrum with sufficient uniformity. The operational wavelength and bandwidth depends on the specifications set by the application, but in general one specifies the 1dB- or 3dB-bandwidth, expressed in nm.
- **Tolerances:** As with many integrated systems, packaging is one of the most complex and costly steps of the entire fabrication process. The coupling to the outside world should therefore be tolerant and robust, to facilitate the pigtailing process. Important tolerance metrics for fiber coupling are positional alignment (typically expressed in micrometer for a 1dB insertion loss penalty), angular tolerances and temperature dependence. Position, angle and temperature can also affect the coupling wavelength and bandwidth.
- **Density:** The off-chip connection density or pin density is an important metric, as the data volumes that need to be transported off-chip are increasing dramatically. While a single fiber can handle a huge bandwidth, the density with which they can be integrated can be important for high-bandwidth applications, or for other applications which require many fibers (e.g. a fiber sensor readout system). Typical fiber arrays consist of a 1-D row of fibers with a pitch of 127µm or 250µm. Coupling solutions with a 2-D arrangement or a higher density will need custom developments and specialty fibers.
- **Chip area:** Given the costs induced by the fab, photomasks and processing steps, the amount of chip area is a costly commodity. The footprint of a coupler can therefore be a significant factor in the cost of the chip, and in some cases the reduction in scale could be severely limited by the fiber coupler solution. A good example is given in [2], where 90% of the silicon photonics chip area is consumed by the couplers to an 8-fiber array.
- **Processing complexity:** Like CMOS processing, the fabrication of silicon photonics is evolving towards process flows where the performance of all components is closely matched. Changes to this process flow to implement a specific coupling solution might impact the performance of other components. This not just for the photonic building blocks, but also for integrated electronics. Therefore, coupler solutions should not violate the design and processing rules of the fabrication flow. For instance, [3] describes the issue of coupling structures penetrating the guard and seal ring and how that affects the choice for a specific coupler. Process complexity also adds to the overall cost and yield equation. Therefore, coupling solutions which require few or no additional processing steps are preferred to solutions which require substantial dedicated (post-) processing.

When discussing various coupling solutions in the next sections, we will evaluate them against these criteria. A summary overview of the performance of the different couplers is given in Table 1 on page 59.

2.3 Polarization Diversity

Because of their high index contrast, silicon photonic wire waveguides are usually very birefringent. The propagation constant for the guided TE mode and the guided TM mode are usually very different [4], and in some situations only one polarization is guided. This means that silicon photonic circuits are usually designed for operation in a single polarization. As already mentioned in the previous section, in many cases the incoming polarization in the fiber is unknown, and a good fiber-chip coupler solution needs to process the light from the fiber in such a way that the operation of the system is as polarization insensitive as possible.

One such approach is polarization diversity, illustrated in Figure 4. Light from the fiber is coupled to the chip and split and the polarizations are physically separated and processed into two different circuits. If a polarization converter is included in the circuit, then the two polarizations could be made identical on the chip, such that the photonic circuits can also be identical. At the output, the outgoing polarizations are combined again using the same

approach. From the point of view of the incoming and outgoing fiber link, the chip appears to be polarization insensitive, while on-chip all circuits operate at a single polarization.

The polarization diversity has some drawbacks, of course: First of all, twice the number of circuits are needed. Due to inevitable variations in the fabrication process, the two circuits will not necessarily function in an identical way. Also, the polarization splitters and rotators might not be 100% efficient, introducing additional losses and even interferometric crosstalk within the chip.

In the next two sections we will discuss the potential of polarization diversity with both edge couplers and grating couplers.

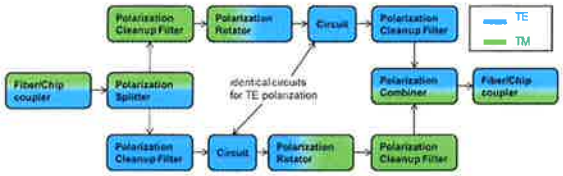

Figure 4: Principle of a polarization diversity approach using a single-polarization on-chip circuit: the polarizations of the incoming light are separated, processed independently and combined again at the output.

3 Edge-coupling solutions

The most straightforward way of coupling light off a chip is by routing it to the edge and butt-coupling it to an optical fiber which is aligned to the axis of the waveguide. This is conceptually illustrated in Figure 5. While it is not necessary to change the propagation direction of the light, the propagation constants should be matched to avoid reflections, and the mode in the waveguide should somehow be expanded to match the mode in the optical fiber.

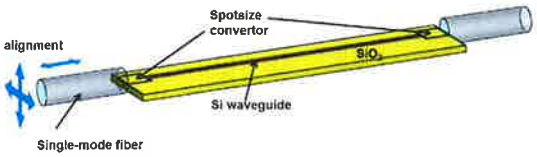

Figure 5: Edge coupling from a chip to an optical fiber.

3.1 On-chip mode conversion

3.1.1 Adiabatic tapers

The easiest approach to accomplish this is adiabatic tapering. By slowly expanding the size of the waveguide core, light will stay in the guided fundamental mode, and the mode size can be expanded until it matches that of a fiber. When the variation is sufficiently slow, there is no problem of reflections or scattering, and if the axis of the taper is straight and aligned with the fiber, there is no need to change the direction of the light: the fiber can be butt-coupled to the larger-core waveguide on the chip.

Figure 6 illustrates a number of possible adiabatic taper solutions for silicon photonic wires. The simplest possible taper just flares out the silicon core in the plane of the chip, which can be easily lithographically defined. This expands the mode in the horizontal direction, but in the vertical direction there is still a significant mismatch.

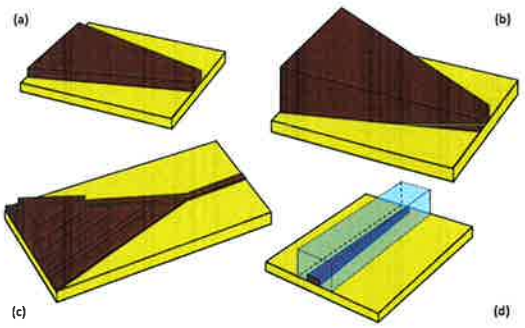

Figure 6: Adiabatic taper geometries for silicon wires: (a) In-plane (2D) taper, (b) linear 3D taper, (c) Staircase taper, (d) inverted taper.

Creating a vertical taper structure is less trivial: an approach as in Figure 6b requires that the layer thickness needs to be gradually changed along the taper's length. This is incompatible with the planar processing technologies used for the fabrication of silicon photonics. An alternative is shown in Figure 6c: by stacking tapered layers, an increasingly thicker waveguide core is built in a staircase geometry [5]. Still, this requires processing of thick silicon layers, which is not necessarily compatible with a CMOS-compatible process flow.

An alternative, much more attractive approach to the 3D tapering problem is shown in Figure 6d. Instead of widening the silicon waveguide core, it is narrowed down into a sharp tip. For narrower width, the core will no longer be able to confine the light tightly, and the mode will expand. A second waveguide core, processed in a lower-index overlay layer (silicon oxynitride [6] or polymers [7]), will take over the confinement of the light.

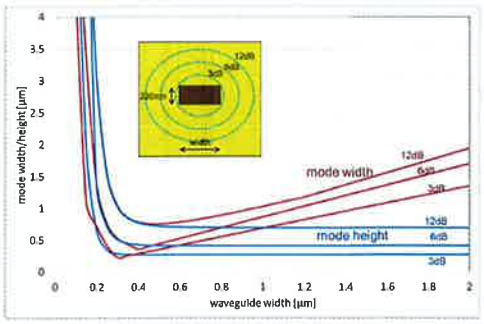

Figure 7: Width and height (3dB, 6dB and 12dB contour of the optical intensity) of the fundamental guided TE mode as function of the width of a 220nm thick silicon wire waveguide. Based on [8], resimulated in Fimmwave.

This inverted tapering approach can be understood more clearly from Figure 7, where the modal width and height is plotted as function of the silicon wire width. We see that for narrow wires the silicon loses confinement, and the mode expands both horizontally and vertically.

Inverted taper-based coupling solutions have been demonstrated with good performance [9]. Insertion losses can be easily lower than 1 dB per coupler [10], [11] and because the mode conversion process is adiabatic, the couplers support a wide wavelength range.

However, inverted tapers are not necessarily easy to make. While the patterning can be done in the same process layer as typical silicon wire waveguides, a narrow tip is required. The best inverted tapers are therefore defined by thermally oxidizing the silicon tip [12] thereby achieving a tip width of less than 15nm.

Also, the inverted taper is only part of the process. It also requires an overlay waveguide with a large core, which is not necessarily easy to define in a planar silicon photonics process,

especially not when several metallization levels are also required. As discussed further, a typical overlay waveguide is a few micrometer thick, which will create a rather large topography on the wafer.

Inverted tapers also require a quite large footprint for the adiabatic mode expansion. Typical taper lengths are between 100µm and 300µm. Most people use linear tapers, but by using optimized taper profiles, the taper length could be reduced somewhat: Close to the wire, where the mode is quite compact, the transition can be faster than in the narrower sections [13], creating a kind of inverted horn [14]. But the footprint is not just dictated by the taper itself: the coupler needs to accommodate the mounting of the fiber, and waveguides need to be routed to the edge of the chip.

3.1.2 Non-adiabatic in-plane mode conversion

Instead of using an adiabatic conversion between the fiber mode and the waveguide mode, one can try to focus the light of the fiber directly into the optical waveguide. A common solution to this is the use of lensed fibers, where the end facet of the fiber is curved to provide a focusing effect. However, such fibers are expensive, and even though the coupling efficiency to a silicon waveguide is much better than that of regular fibers. To obtain high coupling efficiency, the numerical aperture (NA) of the lens should be close to the NA of the waveguide. Even then it will be difficult to obtain a good modal overlap between the focused fiber mode and the photonic wire mode: Due to the high refractive index contrast, the optical mode in the photonic wire has a sharp discontinuity at two of its four interfaces. From a practical packaging point of view, the limited depth of focus now requires an additional alignment step. Even though lensed fibers are regularly used for specialty packaging (e.g. lasers) they add a significant cost to the component.

Instead of performing the lensing in the fiber, one could also consider building the lens on the chip. This is illustrated in Figure 8a. By partially etching a region of a broad silicon waveguide, a planar lens can be constructed, which focuses light into a photonic wire [15]. The performance of this type of structure is quite broadband, with coupling efficiencies between -0.5dB and -2dB.

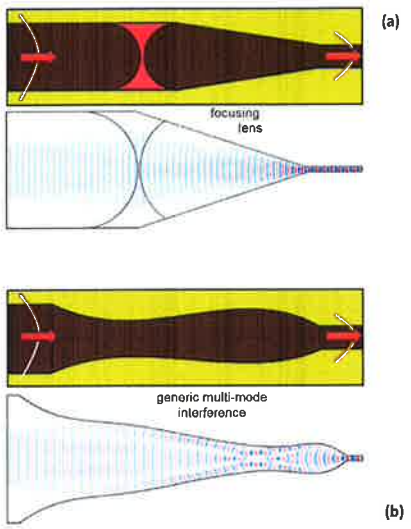

Figure 8: Nonadiabatic in-plane converters. (a) Lens-assisted mode expansion [15] Field plot courtesy of Karel Van Acoleyen. (b) Multimode-interference based mode expansion [16] Field plot courtesy of Bert Luyssaert.

An alternative approach is the use of multi-mode interference. This concept was first proposed by Spühler in [17], where the coupling was optimized by sending the light through a sequence of multimode waveguide sections. The reflections and phase delays of the different modes were tuned such that the resulting field at the output was fiber-matched. An example is shown in Figure 8b. The concept can be extended to waveguides with non-rectangular shapes, where the distinction between the multimode approach and an optimized in-plane lens gradually disappears.

Both approaches discussed here consist of planar mode expanders. As already mentioned, this solves only part of the fiber coupling problem. However, as we will see in section 4 on grating couplers, in-plane mode expanders are still a very useful component.

3.2 Coupling on-chip tapers to fibers

With inverted tapers, and in a lesser extent multimode and lens-based tapers, we can now couple the light from a submicron silicon waveguide to a larger waveguide mode which is better fiber matched. The remaining problem is now to couple this mode to the actual optical fiber. For this, the core of the fiber should be aligned perfectly with the on-chip waveguide. This requires special packaging methods. First of all, the on-chip waveguide has to be terminated in an optically smooth facet, to avoid reflections and unwanted scattering. Secondly, the fiber should be mounted such that the optical axis is aligned with the waveguide and the facets are as close together as possible. As the fiber, with its cladding, has a diameter of about 125µm this means the chip has to be cleaved or polished at the correct position, or mounting structures for the fiber have to be micromachined in silicon chip.

In section 2.2 we mentioned that the commonly used fiber has a mode size of about 10µm. This is quite large to incorporate on a silicon chip, given the amount of topography that would be required for processing. Also, such a large mode needs to be decoupled from the silicon substrate, which is located typically only a few micron below the silicon waveguide level. Therefore, the common solution for end-facet coupling of silicon nanophotonic chips is to use a small-core fiber with a higher numerical aperture. Such fibers have a mode size which is around 3µm. Transition between high-NA fibers and standard single-mode fibers can be accomplished with tapered fibers or even just by a butt-coupled splice. The latter introduces an additional coupling loss of about 0.5dB.

One of the important metrics for fiber coupling is alignment tolerance. As plotted in Figure 9a, the alignment tolerance for a high-NA fiber and matched waveguide is only 0.5µm in all directions for a 1dB penalty [18]. A standard single-mode fiber, coupled to an on-chip waveguide of about 6µm wide waveguide, has about double the alignment tolerance, but with an overall lower insertion loss (Figure 9b).

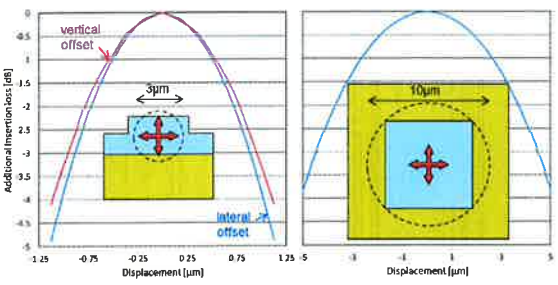

Figure 9: Misalignment penalty on the insertion loss due to fiber misalignment. (a) a 3µm fiber aligned to a 4.5µm silicon rib waveguide, (b) a standard single-mode fiber aligned with a 6µm square waveguide. Measurement data courtesy of Lars Zimmermann, TU Berlin [18].

Aligning optical fibers with a horizontal waveguide is therefore far from trivial. One possible solution is depicted in Figure 10, using silicon V-grooves integrated with the spot-size

converter [19]. Using selective wet etching, V-grooves can be micromachined in the silicon substrate, providing a lithographically aligned support for optical fibers. However, the alignment precision is determined largely by the control of the wet etch process, which can introduce variation larger than the 1dB alignment tolerance of the fiber. More about packaging and fiber-pigtailing is discussed in Chapter 11.

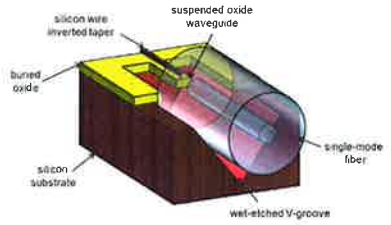

Figure 10: V-groove fiber alignment embedded with inverted taper spot-size converter [19].

3.3 Polarization splitters and rotators

As discussed in section 2.3, any good coupling solution should be able to handle both fiber polarizations, and make sure they are being processed on the chip in the right way. The mechanism of the inverted tapers is in essence polarization-agnostic: the adiabatic tapering converts both the TE and the TM mode of the fiber to the equivalent mode in the silicon waveguide and vice versa. However, as we already mentioned, the silicon waveguides themselves are very polarization sensitive: for most on-chip components, the TE response will be significantly different from the TM response. Therefore, the polarizations should be split, and for an efficient polarization diversity circuit, they should also be rotated.

3.3.1 Polarization splitters

To split the TE and the TM mode in silicon wire waveguides, one can again use various mechanisms. As we want to split two modes with a very different propagation constant, we can use multimode interference in a directional coupler to split the two polarizations: By designing the waveguides such that the beat length in the directional coupler for TE and TM are a non-integer fraction (e.g. 3/2, 5/3,…), the length of the coupler can be designed such that the TE mode is coupled to one waveguide and TM to the other waveguide. However, the beat length of both modes is very dependent on the geometric parameters of the waveguides, and the interferometric nature of the component also makes it wavelength-sensitive, partially negating one of the benefits of the inverted taper coupler.

A more elegant approach is to make use of the difference in confinement between the TE and TM modes using a directional coupler. By making the gap between the waveguide in the directional coupler sufficiently large, we can make sure that only the lowly confined TM mode couples to the neighboring waveguide while the highly confined TE mode stays in the same waveguide. This approach, illustrated in Figure 11a, is simple in its concept and since the confinement is not very wavelength dependent, is a more wavelength insensitive approach to split the polarizations than the purely multimode interference based directional coupler [20], [21].

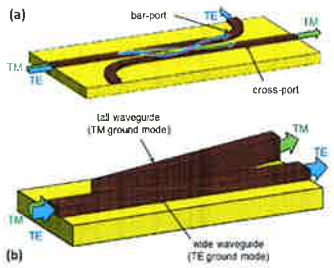

Figure 11: Polarization splitter components. (a) Directional coupler based [22], (b) Mode-evolution based polarization splitter based on [20].

An alternative is again an adiabatic transition. In a so-called mode-evolution polarization splitter, the shape of the waveguide is gradually changed such that the TE and the TM light preferentially reside in a different section of the waveguide. The TE mode is the ground mode of the original waveguide, where the core width is larger than the height. Likewise, the ground mode of a thicker but narrower waveguide will have a TM nature. By adiabatically introducing such a vertically oriented core in the vicinity, TM light will migrate to the second core and TE will stay in the original core.

3.3.2 Polarization Filter

A polarization splitter is never perfect and a commonly used figure of merit besides the insertion loss is the ratio of transmittance (typically expressed in dB) between the polarizations in the output ports or the *polarization extinction ratio* (PER).

In order to improve the PER one can use a polarization clean-up filter [23]. A straightforward solution would be to cascade several polarization splitters with a resulting PER improvement in proportion with the number of polarization splitters. An alternative which is especially interesting to filter out the TM mode, is to use a waveguide section such as a rib waveguide which only guides the TE mode and in that way radiates away the unwanted TM mode. Similarly, a waveguide bend with a sufficiently small bending radius will have a higher loss for the TM mode than for the TE mode.

3.3.3 Polarization Rotators

The polarization splitter is only part of the solution for a polarization diversity circuit. One of the polarizations (mostly TM) now needs to be converted to the main on-chip polarization (typically TE). For this a polarization rotator is needed. Typically one prefers to perform the routing functionalities in the TE mode since the bending radius can be taken very small (around 5μm) without introducing exuberant losses. Again, the rotation can be accomplished using different mechanisms, with adiabatic transitions and multi-mode interference being the most common solutions. As with the polarization splitters, adiabatic polarization rotators are based on the principle that the TE mode is the ground mode of a 'horizontal' waveguide core, while the TM mode is the ground mode of a 'vertical' waveguide core. An adiabatic polarization rotator tries to gradually 'rotate' the core. Note that simply changing width and height of the core will not work: The TE-polarized light will remain in the TE mode, even if it is no longer the ground mode, and likewise for the TM-polarized light. A symmetry-breaking is required to actually rotate the polarization. As twisting a rectangular core is difficult to accomplish in a planar fabrication process, alternative geometries are required. An example is shown in Figure 12a [24], [25], [26].

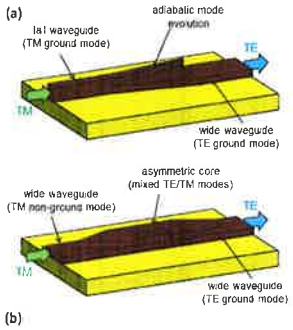

Figure 12: Polarization rotator geometries. (a) Adiabatic mode-evolution rotator [24], (b) multimode interference polarization rotator [27].

Polarization rotation can also be accomplished using multimode interference. The simplest form is just using 2 modes, as in a directional coupler. To accomplish polarization rotation, the TE and TM polarization should be coupled into a waveguide with two orthogonal modes which have a 50/50 mixed polarization state. Again, one needs to break the symmetry of the waveguide for this purpose. This was proposed in [28], using a partially etched cladding positioned with an offset to the silicon waveguide core. A more fabrication-friendly approach, which does not require a special cladding material, is shown in Figure 12b [27]. A partial etch of the waveguide also creates an asymmetric waveguide with 2 hybrid TE/TM modes with different propagation constants [29]. By choosing the length of this waveguide correctly, the beating between the two modes will result in a coupling from the TM to the TE mode (and the other way around). The efficiency of these components can be very high, up to -0.5dB or higher, and very broadband. Typically one characterizes a polarization rotator using the insertion loss and the *polarization conversion efficiency* (PCE), i.e. the fraction of transmitted light that ends up in the correct polarization.

3.4 Edge coupling: conclusion

The most straightforward coupling solution for silicon photonic chips is edge-coupling. This has been the standard for photonic integrated circuits in many material systems, and it can be applied to silicon as well. Inverted tapers provide a simple and efficient coupling mechanism that, when combined with on-chip polarization splitters and combiners, enables broadband, polarization insensitive coupling between fiber and silicon waveguides.

The main difficulty with edge coupling lies in the post-processing and packaging. Silicon wafers have to be diced, and facets need to be cleaved, polished or micromachined before the fiber can be attached. This is a significant drawback in a wafer-scale manufacturing system, as it precludes wafer-scale testing of the photonic components.

4 Surface Couplers

In electronics, the standard way to contact the electrical circuits is through metal pads on the top surface of the chip. This allows for wafer-scale testing by probing the individual chips on the wafer or even the entire wafer itself without need for intermediate packaging or post-processing steps. As discussed in the previous section, edge coupling does not provide this advantage, so for photonics an alternative strategy is needed that allows vertical coupling of light to and from the chip. This will enable wafer-scale testing.

Also, surface couplers introduce several other advantages: The density of optical 'pins' can be much higher. The couplers can be positioned anywhere on the chip (especially those for testing) and do not need to be routed to the edge. Chips can be probed with fibers oriented at an angle close to the vertical.

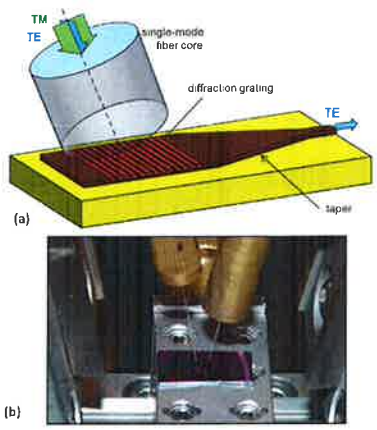

Figure 13: Grating coupler. (a) Principle: light from a (near-) vertical optical fiber is diffracted into the waveguide. (b) Grating-coupler based measurement setup with two fibers.

However, there is one considerable challenge in surface coupling. Light needs to make a dramatic change in direction from the on-chip waveguide to the fiber. And as with edge couplers, the mode size mismatch needs to be overcome as well.

The most common solution to this problem is the grating coupler: a diffraction grating is designed such that all the scattered contributions interfere constructively in a vertically radiated wave which is as much as possible fiber-matched. This is shown in Figure 13. In the past decade, the grating coupler has established itself as the standard solution, but with a large variety of flavors based on different fabrication strategies or applications. These are discussed in detail in the following section.

Grating couplers are not the only way of achieving surface coupling to a fiber. There exist some alternatives which are used for specific (research) applications, and these are briefly discussed in paragraph 4.7.

4.1 Grating couplers: operating principle

A grating coupler consists of a periodic refractive index modulation in or close to the waveguide core. In silicon photonics, grating couplers are most often implemented as etched grooves in the silicon waveguide core [30–32]. Every such groove acts as a scatterer. Other ways to implement a refractive index grating is by adding metal lines [33] or etching subwavelength features that act as an effective medium [34–37]. When light is incident from the waveguide on the chip, some combinations of wavelength, grating period and off-chip angle will cause all scattered contributions to be in phase, and thus a coherent phase front radiates away from the chip. This condition called the *Bragg* condition, illustrated in Figure 14a, occurs when the phase delay between the diffraction of two adjacent grating teeth is exactly 2π (or a multiple thereof). For the directions where this phase condition is not met, the contributions of all the grating teeth will interfere destructively.

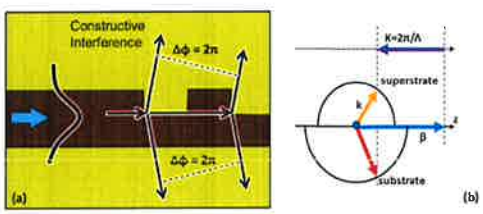

Figure 14: Operational principle of a grating coupler. (a) Phase fronts in real space, (b) K-vector diagram.

An alternative way of calculating the operating condition for a grating coupler is in k-space, shown in Figure 14b. A periodic structure like a diffraction grating carries its own impulse $K=2\pi/\Lambda$, which can be transferred to the photons in the waveguide. The conservation of momentum in the z-direction therefore dictates that $k_z = \beta + m K$ ($m = 0, \pm1, \pm2, ...$).

Shown in Figure 14b, there is a solution for m=1. While in the out-of-plane direction, the nonperiodic structure of the waveguide does not pose any restrictions, except that the magnitude of the k-vector in the top and bottom cladding should match $k = n_{clad} \cdot k_0$.

We see that for light from the waveguide, there are in general two solutions, an upward and a downward radiating wave. The respective angles of these waves depend entirely on the material index of the top and bottom cladding material. The fact that there are two solutions poses a problem for the coupling efficiency: somehow the light must be forced into the direction of the fiber, and not the substrate. Solutions for this are discussed further in section 4.2.

For a given wavelength and cladding material, the period of the grating determines the outcoupling angle. For a perfectly vertical angle, we find that the grating period Λ relates to the optical wavelength λ as $\Lambda = \lambda / n_{eff}$, with n_{eff} the average refractive index of the grating which can be approximated by a linear relationship (a weighted average of the etched and the unetched region) according to the coupled mode theory, as the wave is propagating in the fundamental mode in the grating [38]. This situation for vertical coupling, shown in Figure 15b, is called a second-order grating, because there is now also a solution for m = 2: The grating can now reflect light back into the waveguide. This makes diffraction gratings somewhat less suitable for pure vertical coupling, and most practical grating couplers use a coupling angle of 9° to 12° off the vertical. This can be either forward coupled, using a period which is larger than the pure second-order period (Figure 15c) or backward coupled, with a sub-second-order grating (Figure 15a). This problem with vertical coupling can pose a problem for efficient pigtailing, but also for the integration of components which require true vertical coupling, such as VCSELs. Possible solutions for true vertical coupling are discussed in paragraph 4.3.

In the case of the commonly used 220nm thick silicon core, the effective index of the core is about 2.8 for a wavelength of 1550nm and TE polarization. For a 70nm etch, the effective index is about 2.5. A true second-order grating would therefore have a period of 590nm. Forward coupling at 10° would require a period of 630nm [39], while backward coupling would require a period of 545nm.

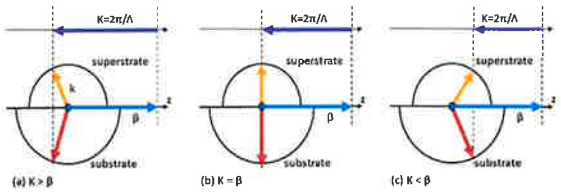

Figure 15: Grating coupler with different period (a) < 2nd order, (b) exactly 2nd order, (c) > 2nd order.

The Bragg condition only describes an infinitely long grating, and does not take into account the other requirements for efficient fiber coupling. In a finite grating, every grating tooth will scatter some light, reducing the remaining light in the waveguide. This, in effect, causes an exponential decay of the power in the waveguide mode. Also, at the first teeth the grating is not yet a fully periodic structure, so some scattered light of those first teeth will not combine with the coherent flat phase front radiated by the rest of the grating. This is shown in the radiated field plot in Figure 16. Obviously, the exponential decay in the waveguide will also induce an asymmetry in the radiated wave. The overlap of this wave with the symmetric optical fiber mode will therefore be far from perfect. An approach to improve this overlap is discussed in paragraph 4.2.

Note that there is an equivalence in describing a grating coupler from the fiber point of view or from the waveguide point of view. As the coupling efficiencies are always expressed as mode-to-mode coupling, they are always bidirectional.

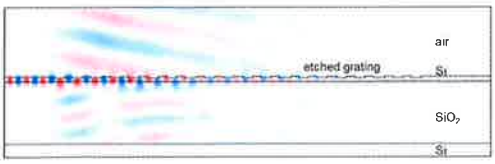

Figure 16: Field plot of an etched grating coupler, illustrating the effect of the first grating teeth and the exponential decay of light in the waveguide. The grating coupler is designed in a 220nm silicon layer with a 70nm etch, and a period of 630nm [31].

The finite size of the grating coupler has another effect: Depending on the exact parameters, there will be about 12 to 20 periods covering the size of the fiber core. Because the number of scattering point is relatively small, and the scattering cross section of each tooth is relatively large, the Bragg condition will exhibit a relatively large bandwidth. This is shown in Figure 17b. The typical grating coupler from [31] has about 5dB (30%) peak coupling efficiency, and a 3dB bandwidth of about 60nm. Similar numbers have been reported by [40–42], with coupling efficiencies going close to 50%. While the bandwidth is large compared to classical low-contrast gratings [43], it is small compared to the hundreds of nm reported for edge couplers. In many cases a larger bandwidth is required, or even several wavelength bands need to be coupled. This is discussed in some more detail in paragraph 4.6.

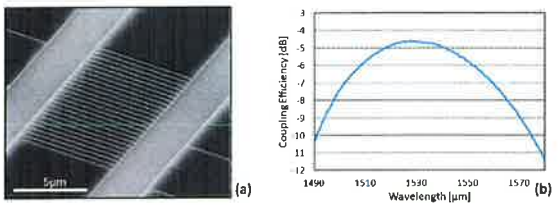

Figure 17: The grating coupler simulated in Figure 16. (a) SEM micrograph, (b) Measured coupling spectrum for a fiber at 10° [31].

Unlike a typical edge coupler, grating couplers couple directly to a single mode fiber, with a core size of about 10μm. Therefore, the tolerances for misalignment are higher than for the edge coupler. This is shown in Figure 18a. The lateral misalignment tolerance for 1dB coupling penalty is larger than 1μm. In the longitudinal direction, it is even better, but in Figure 18b we do see a shift in peak wavelength as we move the fiber along the axis of the on-chip waveguide.

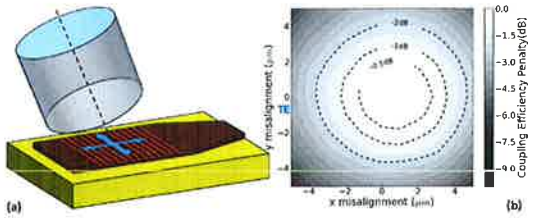

Figure 18: Misalignment tolerances for the grating coupler in Figure 16 and Figure 17. Measurement data courtesy of Michael Vanslembrouck.

As already mentioned several times throughout this chapter, the small silicon waveguides are strongly birefringent. This means the Bragg condition for the TE and the TM waveguide mode will be very different, and a grating coupler designed for a given wavelength and coupling angle will therefore only work for a single polarization, either TE or TM. Approaches to address this issue and still enable polarization diversity on a chip, are discussed in paragraph 4.4.

The one-dimensional line gratings, as described here and shown in Figure 13, couples light from a fiber to a waveguide whose width is fiber-matched. This is typically 10µm or wider. This waveguide still has to be tapered down to a single-mode wire waveguide. While the grating coupler itself can be quite compact, a linear taper should be at least 150µm long. Solutions to this problem are discussed in paragraph 4.5.

4.2 Optimizing grating coupler efficiency

The simple grating coupler presented in the previous paragraph has a coupling efficiency of about 30% (-5.22dB). While this is good enough for most research purposes, better coupling is required for most real-world applications: a high coupling loss is not only detrimental to the overall power budget, but the light that is not coupled correctly can give rise to crosstalk elsewhere on the chip.

The coupling efficiency of the grating coupler is determined mainly by *directionality* and *modal overlap*. When looking from the perspective of the waveguide, the light needs to be sent as much as possible into the right diffraction order, i.e. the first order upward diffraction. Also, reflections have to be minimized. Once diffracted, the field profile should match as much as possible the mode of the optical fiber at the correct angle.

4.2.1 Improving directionality: Bottom mirror

In a regular (near-)second-order grating coupler, the Bragg condition has two solutions: an upward and downward radiating wave. Somehow, that unwanted downward wave should be suppressed or redirected in the upward direction. This can be accomplished by incorporating a mirror in the substrate. In effect, a silicon-on-insulator substrate already has such a mirror embedded: the interface between the buried oxide (BOx) and the silicon wafer. This is shown in Figure 19a. Specular reflection at this interface is around 17% for a wave incident at 10 degrees. So without any special tricks, there is already a fraction of downward radiated light being recycled.

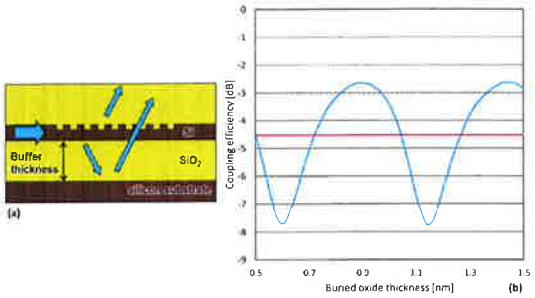

Figure 19: Reflection at the buried oxide interface (a) Principle, (b) Coupling efficiency at 1550nm and 8° angle as function of buried oxide thickness [44] Simulation data courtesy of Dirk Taillaert.

However, the reflected wave will interfere with the original upward wave, so the effect of the recycling can be either positive or negative. To maximize the upward coupling efficiency, the interference should be constructive. This can be accomplished by choosing the right thickness of the buried oxide, to tune the path length difference between the upward and the reflected wave. Figure 19b shows the simulated coupling efficiency of the grating coupler in Figure 16 for a changing thickness of the BOx layer. Coupling efficiencies can vary from -2.7dB and -7.5dB between the best and worst oxide thickness. We also see that the 2µm buried oxide used by many groups is not optimal for grating couplers operating at 1550nm.

The effect of the buried oxide can be enhanced by incorporating a more efficient reflector in the substrate. Two examples are shown in Figure 20. Instead of a single interface, a distributed Bragg reflector can be embedded [45], [46]. Of course, building such a reflector in an off-the-shelf SOI substrate is not possible. Therefore, in this case, all layers, including the waveguide layer, consist of PECVD deposited amorphous silicon and oxide. Coupling efficiency of this grating coupler is close to 70% (-1.6dB).

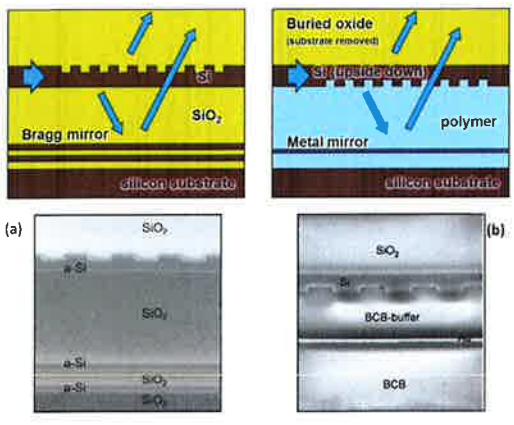

Figure 20: Grating couplers with a bottom mirror (a) Grating coupler in deposited amorphous on top of a DBR mirror stack [45]. SEM picture courtesy of Shankar Kumar Selvaraja (b) Bonded grating with gold 'bottom' mirror [47]. SEM picture courtesy of Frederik Van Laere.

While amorphous silicon can have relatively low losses [48], it is not straightforward to integrate active components in it. Therefore, an alternative way to add a bottom reflector a standard silicon substrate is to use a bonding technique. First, a top oxide and reflector is deposited, and subsequently the entire structure is bonded upside down onto a carrier, after which the original substrate is removed. The top mirror then becomes a bottom reflector. An example, making use of BCB and a deposited gold mirror, is shown in Figure 20b [47]. The coupling efficiency, at 69%, is comparable with that of the DBR mirror in amorphous silicon. The top mirror can also be processed in silicon, as demonstrated in [49].

4.2.2 Improving directionality: Grating profile optimization

Adding a mirror under the grating is an effective way of improving the grating coupler directionality, but it is far from straightforward from a fabrication point-of-view. Therefore, instead of trying to recycle the downward radiated light, we can try to suppress the downward diffraction order altogether. This can be done by optimizing the grating profile. The general principle is shown in Figure 21a for an etched grating: the main scattering points within one period are located at the corners of the etch profile. By now tuning the tooth width and depth, the phase difference between the upward components is 2π, while between the downward components it is π. This way, the downward diffracted wave will experience significant destructive interference and will be much weaker than the upward wave [50]. From a Fourier optics point of view [51], [52], one can see the grating as a binary phase grating which is different for downwards diffracted light and for upwards diffracted light. For the downward diffracted light, the grating is a zero-phase grating which means that the first diffraction order is suppressed. For the upwards diffracted light, the grating behaves as a π-phase grating such that only uneven diffraction orders exist. This just illustrates the principle, because of the high

refractive index contrast, the grating has to be numerically optimized. This results in a grating teeth that are thicker than the standard silicon waveguide core. Therefore, to fabricate such an optimized grating, additional fabrication steps are needed.

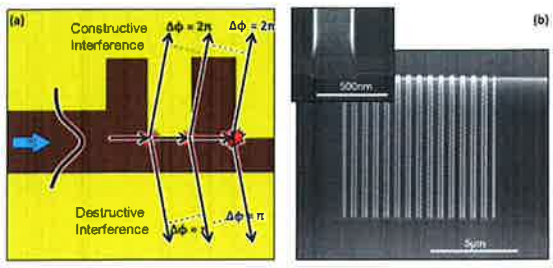

Figure 21: Improving the directionality by optimizing the grating profile [53]. (a) principle, (b) fabricated grating

To implement a thicker grating, additional silicon needs to be added. This can be done using epitaxy, and experiments show indeed an improved grating performance from 30% to 55% [54]. However, it is not straightforward to control the tooth profile using epitaxy. Alternatively, the grating top layer can be deposited and subsequently etched [53], [55]. Using an amorphous or polysilicon and embedded etch-stop layers, a better control of the grating profile is possible. Coupling efficiencies of 70% have been reported [32], [56]. The grating overlay does not have to be silicon but can be any material such as SiN [57], as long as it introduces a π-phase difference. Another approach is to start with a thick silicon core and etch the grating and entrance waveguide using an inverted taper [58], [59].

4.2.3 Improving modal overlap

The overlap of the diffracted wave with the optical fiber mode is determined by the lateral mode profile and the longitudinal mode profile. The lateral mode profile of the ground mode of a broad high-contrast silicon waveguide closely resembles a cosine with very small evanescent tails. The profile of the optical fiber is more Gaussian-like, with more extended tails. However, by just optimizing the silicon waveguide width, a 1D modal overlap of almost 100% can be obtained, without any further engineering.

In the longitudinal direction, we've already shown in Figure 16 that there is a significant mismatch between the exponentially decaying intensity profile in the waveguide and the Gaussian-like fiber mode. The maximal overlap between the exponential decaying field of a uniform grating and the Gaussian profile of the fiber is 80%. This provides much room for optimization.

The exponentially decaying field profile is induced by periodically scattering a fixed fraction of the remaining light in the waveguide. Therefore, to change the exponential profile into a more fiber-matched profile, we need to tune the amount of scattered light in each grating tooth, as shown in Figure 22a. The first grating teeth should only minimally scatter, most of the light should be scattered in the center, and the remaining light should be diffracted at the end. Also, the overall diffraction strength of such an apodized grating should be such that there is no more light remaining in the waveguide at the end of the grating. Tuning the scattering cross section of each individual tooth can be accomplished by changing the width and depth. The latter is difficult to achieve directly, unless one makes use of local etching techniques such as focused ion beam (FIB) writing or by utilizing the lag effect in the dry etching process [60]. Changing the width can be done lithographically, but as the narrowest lines are typically well below 100nm in width, very good patterning (e-beam) is required to make such gratings. A simulated field plot of such an optimized grating is shown in Figure 22b, and gratings with coupling efficiency up to 75% have been demonstrated in combination with a silicon overlay or thick core waveguide grating [32], [61], [62].

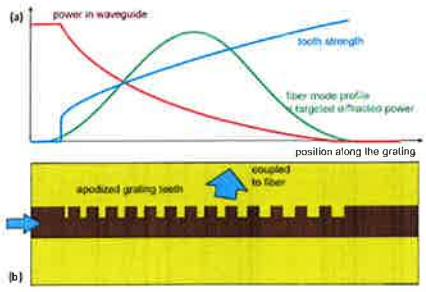

Figure 22: Optimizing modal overlap by apodizing the grating [30]. (a) optimizing the scattering profile, (b) schematic drawing of apodization by changing the trench width.

4.3 Grating couplers: true vertical coupling

When we considered the Bragg condition for perfect vertical coupling in paragraph 4.1, we noticed that there appeared an additional solution for the second-order diffraction: back into the silicon waveguide. While many solutions can get by with tilted fibers, vertical coupling facilitates matters considerably, and also enables coupling from vertical emitters, such as VCSELs. Reflections are not only a problem when the light comes from the waveguide. The light from the fiber will also be partially reflected, as the 0^{th} order backward diffraction (which is specular reflection) is sent back into the fiber. Also, from the fiber point of view, a simple periodic grating will not introduce a preference for "forward" or "backward" coupling: the light of the fiber is essentially split in two. This can be alleviated by breaking the symmetry, such as in the apodized grating discussed in paragraph 4.2.3 [63] or with a slanted grating [64].

A simple solution to obtain efficient vertical coupling is to "trick" the grating into non-vertical coupling and subsequently redirecting the diffracted light in the vertical direction. This can be easily accomplished by adding a refractive interface at an angle, as shown in Figure 23a. Such a wedge is not straightforward to make, as it is a 3-dimensional structure. Figure 23b shows such a wedge in polymer fabricated by imprinting a UV curable polymer with a focused-ion-beam fabricated mold [65]. Alternatively, one can use an angled fiber for vertical fiber coupling as shown in [66].

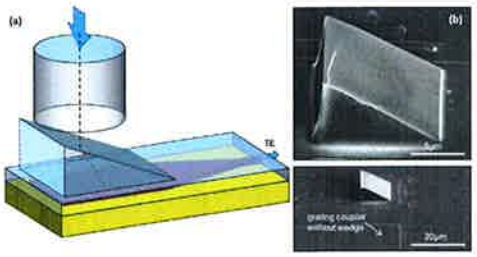

Figure 23: Vertical coupling using a wedge on the grating. (a) principle, (b) fabricated structure with a polymer wedge. SEM pictures courtesy of Jonathan Schrauwen.

It is also possible to reduce the reflections by adding an additional reflecting structure. This might seem counterintuitive, but if the phase delays are constructed properly, both reflections can interfere destructively, resulting in a higher transmission. In Figure 24 this reflector is fabricated by a deep-etched slit in the waveguide [50]. To get the phase delays right, the width and the position of this slit must of course be accurately controlled. This type of reflector also introduces a symmetry-breaking, which results in a highly preferential coupling from the vertical fiber into one waveguide direction.

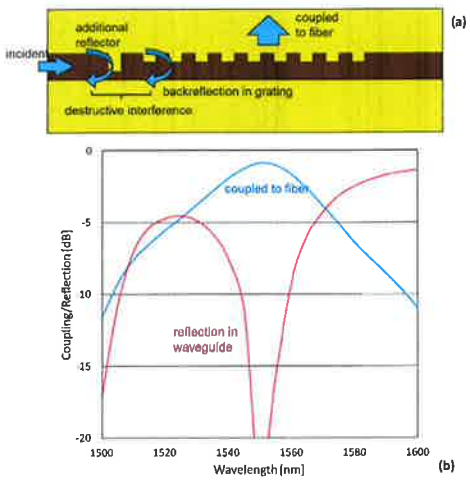

Figure 24: Vertical coupling using an additional reflector in front of the grating [50] (a) Principle, (b) Coupling efficiency and reflection as function of wavelength.

4.4 Grating couplers and polarization

Because of the birefringence of the silicon waveguide, The Bragg conditions at a given wavelength and angle will only be satisfied for a single polarization. As the TE polarization is the most commonly used in silicon waveguides (as it is the fundamental mode when the core width is larger than the thickness), all grating couplers discussed up to this point are designed for the TE polarization. However, it is also possible to design a grating coupler for the TM polarization. For the regular 220nm thick SOI layer, the effective index for the TM mode is 1.85, compared to the TE index of 2.8. When using a 70nm deep etched grating (same value as for TE, but not optimized for TM), this will result in a grating period of 1040nm. Coupling efficiency for such a grating is somewhat lower than for TE at about 20% [67].

However, for many applications both fiber polarization needs to be coupled at the same time, and to enable a polarization diverse circuit, these polarizations need to be physically split into different circuits. In this section, we will discuss two solutions to this problem: using a 2-dimensional grating coupler, which acts as a polarization splitter, and using 1-D grating couplers tuned to couple both polarizations.

4.4.1 2D polarization-splitting grating couplers

The 1-D grating shown in Figure 16 couples the TE polarization efficiently to the slab waveguide. However, from the point of view of a vertically oriented fiber, there is no difference between the two polarizations. Therefore, a 1-D grating oriented at a right angle to the original grating coupler will couple the other fiber polarization. Overlaying the two 1-D grating profiles will result in a 2-D grating which can be patterned as a matrix of etched holes [68]. This principle is shown in Figure 25a.

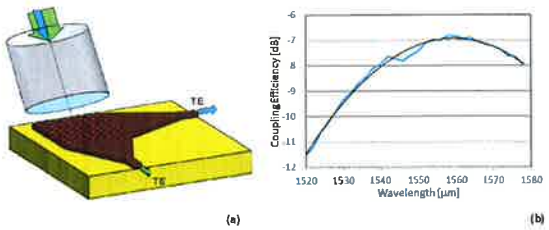

Figure 25: 2-D grating coupler [69] (a) Principle, (b) Coupling efficiency spectrum.

However, as we already discussed, a grating designed for a perfectly vertical fiber has the drawback of introducing unwanted reflections. Therefore, we prefer to slightly tilt the fiber.

While for a 1-D grating this just shifts the Bragg condition, for a 2-D grating it also breaks the symmetry between the two polarizations. This will result in a slightly reduced rejection ratio and introduce some polarization-dependent loss for the overall chip [70]. Also, the change in the Bragg condition with a tilted fiber requires that the waveguides on the chip are no longer at a right angle [71]. Alternatively, one can keep the waveguides at a right angle and use tilted grating instead. However, even then it is not possible to fully decouple the polarizations with a tilted fiber. With a vertical fiber the polarizations are perfectly decoupled, but then an additional symmetry is introduced: Each polarization can now be diffracted forward or backward. This is OK for some receiver applications [23], [72], but in many situations it is preferable to have the light of each polarization in one waveguide, not two.

Figure 25b shows the coupling efficiency for a 2-D grating coupler for both the TE and the TM polarization in the fiber. We see that the coupling efficiency is slightly lower than for the 1-D grating which can be attributed to the nonoptimized etch depth.

Such grating couplers have been used to demonstrate polarization-diversity circuits with moderate polarization-dependent loss [73]. However, for tilted fibers the PDL is only low near the peak coupling wavelength. This is shown in Figure 26. In order to reduce the PDL for a broader wavelength range, one has to use more complex shape holes instead of circular holes. This will successfully reduce the PDL to a minimum over the whole bandwidth of the 2-D grating coupler [32].

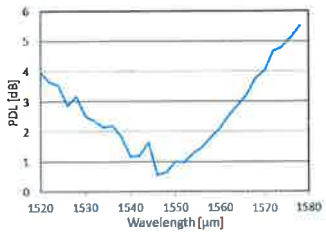

Figure 26: Polarization dependent loss for a polarization-diverse circuit with 2-D grating couplers [70].

4.4.2 1D polarization-splitting grating couplers

As explained in section 4.1, there is a fixed relation between the grating period, the wavelength, the effective index of the waveguide mode and the angle of the fiber. As the effective index for the TE and TM mode of the slab waveguide is different (TM mode has a lower effective index), they will diffract at a different angle for a given grating and wavelength. One can now choose the grating design such that the angle of the TE waveguide mode is positive (forward coupling) and that of the TM waveguide mode is negative (backward coupling), but with the same deviation from the vertical. This is illustrated in Figure 27a. If we now reverse the situation, and look at it from the perspective of the fiber (Figure 27b), the TE polarization will be coupled forward, while the TM polarization will be coupled backwards [46], [74–76].

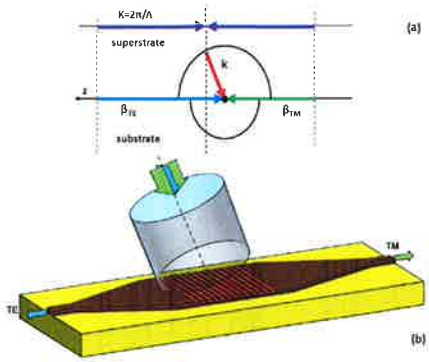

Figure 27: Principle of the 1D polarization splitting grating. (a) k-vector diagram (from the perspective of the waveguide, (b) polarization splitting function (from the perspective of the fiber).

If we go through the math for a silicon slab waveguide of 260nm thick at a wavelength of 1550nm, with an effective index of 2.87 for TE and 2.1 for TM, we can plot the coupling angle of the fiber as a function of grating period (for 70nm etch) in Figure 28a. We find that the absolute value of the coupling angle of the fiber is 15° for both polarizations when the grating period is 630nm [75].

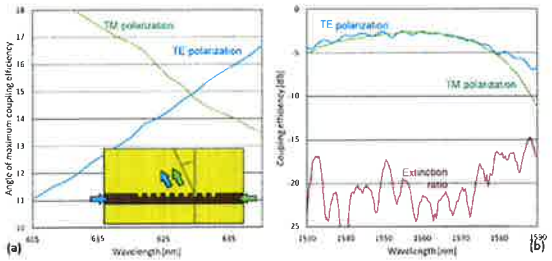

Figure 28: 1D polarization splitting grating. (a) Coupling angle for TE and TM mode as function of grating period, with a crossing at 630nm and an angle of 15° (b) Measured coupling efficiency of both polarizations for this situation [75]. Data courtesy of Zhechao Wang, Yongbo Tang and Sailing He, KTH.

Figure 28b shows the measured coupling efficiency of such a device [75], where both polarizations show a similar insertion loss of around -3dB, with an extinction ratio of over 10dB.

A drawback of this approach compared to the 2-D grating is that an additional polarization rotator is required to obtain identical polarizations in the two waveguides. We already discussed such components in paragraph 3.3.3**Error! Reference source not found.**

4.5 Grating couplers: Reducing the footprint

The grating couplers we have discussed up till now couple light from a fiber into a broad waveguide. This means an additional mode size converter is required to laterally compress the light into a narrow photonic wire waveguide. An adiabatic taper for this purpose is typically 150µm long, but we have discussed more compact taper solutions in paragraph 3.1.2.

However, it is possible to combine the function of the grating and the in-plane converter by moving away from a straight-line grating and instead use the grating diffraction itself for in-plane spot-size conversion. By curving the grating lines, the grating will act as an in-plane diffractive lens [77]. The principle is explained in Figure 29a. Instead of a global Bragg condition, the condition is calculated locally, such that the light from the fiber is diffracted towards a single point. This results in elliptical grating lines with a common focal point. The focusing distance can be quite short, but the ellipse segments should still have a significant overlap with the fiber mode. In practice, the focusing distance can be less than 20µm without a significant penalty on the insertion loss, and a very short taper can be used. Such a short grating is shown in Figure 29b.

Actually, because the grating focuses the light itself, the taper structure is not necessary. Figure 29d shows a curved grating etched in a slab waveguide, with only a waveguide aperture at the focal point [77]. Similar coupling efficiencies are measured for both types.

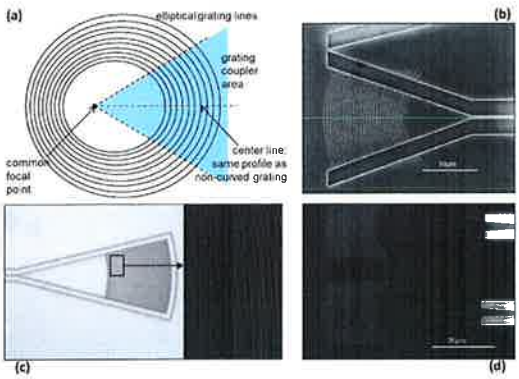

Figure 29: Curved grating coupler (a) Principle of the curves, (b) Focusing grating coupler in a waveguide taper [77]. Image courtesy of Frederik Van Laere (c) a similar device from [32]. Image courtesy of Attilu Mekis, Luxtera. (d) Focusing grating coupler in a slab waveguide with a collection waveguide opening in the focal point [77]. Image courtesy of Frederik Van Laere.

Because the Bragg condition can be tuned locally by changing the grating curves, there is no more the requirement that the fiber and the on-chip waveguide are in the same vertical plane. For this, only the orientation of the ellipses needs to be changed with respect to the coupler [78]. This will not improve the coupling efficiency in any way, but the advantage is that the grating will now no longer reflect in a specular way, back into the on-chip waveguide.

Such an off-axis grating also makes it possible to implement a 2-D polarization-splitting grating coupler, by overlaying two off-axis elliptical gratings, and etching a correctly sized hole at the intersection of the grating lines [50]. Such a device is shown in Figure 30.

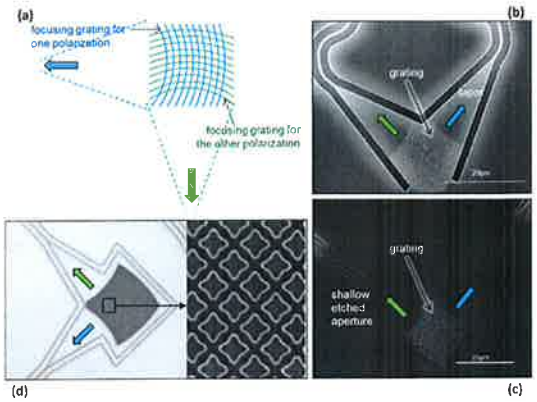

Figure 30: 2-D Curved grating coupler (a) Principle and (b, c) SEM picture of fabricated structures [79]. Images courtesy of Frederik Van Laere. (d) A similar device from [32]. Image courtesy of Attila Mekis, Luxtera.

4.6 Grating coupler bandwidth

Grating couplers are diffractive structures, and the coupling conditions derived in section 4.1 clearly show a wavelength-dependent behavior. Still, because the grating has only a limited number of periods (to fit in the mode size of a fiber) and the individual scatterers quite strong, the 3dB bandwidth of the grating is still of the order of 60-80nm. Increasing the bandwidth is possible by reducing the number of grating teeth and at the same time increasing the strength of the scatterer. In silicon, this is difficult without shrinking the grating: the bandwidth will increase, but the overall coupling efficiency will drop dramatically because of the smaller overlap with the mode of a single-mode fiber.

To have fewer teeth, but still retain a good overlap with the fiber mode, the period of the grating should increase. As the period of the grating is linked with the Bragg condition, this implies that the effective refractive index of the grating should be lowered. This is difficult in silicon, but grating couplers in silicon nitride have been demonstrated, with 1dB bandwidths of around 100nm [80], [81].

However, there is one particular situation where a silicon grating coupler can add additional bandwidth by using both the forward and the backward diffraction. As with the 1-D polarization splitter discussed earlier in paragraph 4.4.2, it is possible to design the grating in such a way that the Bragg condition for the forward and backward wave matches the same fiber angle, in this case for two different wavelengths [82]. This is shown in Figure 31, where the grating coupler is designed to couple a wavelength band between 1490nm and 1550nm, and another band around 1310nm.

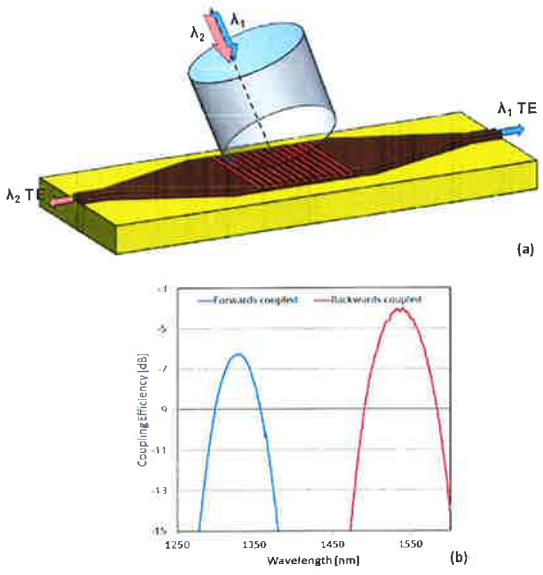

Figure 31: Grating coupler + wavelength duplexer [83]. (a) Principle (b) Measured coupling efficiency for the 1550nm and 1310nm wavelength band.

4.7 Alternative surface coupling solutions

Even though grating couplers are now the most commonly used vertical coupling scheme, there are some alternatives that we will briefly discuss here.

4.7.1 Grating coupler fiber probe

In this entire section, we considered a grating coupler which was integrated in the waveguide on the optical chip. However, there is no requirement that the grating should be physically attached to the waveguide: As long as the grating is sufficiently close to the waveguide for the waveguide mode to feel the teeth, there can be coupling.

Instead of mounting the grating coupler on the chip, it can be mounted directly on the fiber [84], [85], as shown in Figure 32. Using a polymer curing technique and undercut, a gold grating is transferred to the fiber facet, but at an angle to keep the grating parallel with the chip surface [84]. This can even be done with polymer curing using UV light transmitted through the fiber core, which results in a very compact, self-aligned probe.

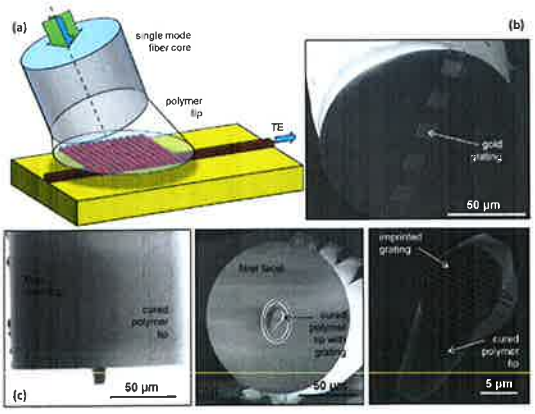

Figure 32: Grating coupler fiber probe with gold mirror on the fiber facet. (a) Principle (b) Fiber facet imprinted with grating coupler. (c-e) Fiber facet with core-only cured polymer facet [84].

Coupling efficiency for such a fiber is somewhat less than with a regular grating, and the fact that the distance between the grating and the waveguide cannot be controlled with the same accuracy as an etch grating, makes the coupling strength less reproducible. However, the coupling spectrum is similar to that of a regular etched grating or a gold grating fabricated on a waveguide.

The important advantage of having the grating on the fiber instead of on the waveguide is that the chip can now be probed on any location with a suitable waveguide: there is no need for dedicated fiber couplers on the chip; this means that components within a circuit can be individually probed to test their response. The requirement is of course that a sufficiently broad waveguide section is foreseen.

4.7.2 *Evanescent fiber coupling*

A coupling scheme with similar benefits is to use evanescent coupling between an optical fiber and an on-chip waveguide. Because the optical fiber is much larger, and protected by a cladding, it is thinned down by heating and drawing the fiber [86]. When correctly tapered down, the original cladding will now become a core with a significant fraction of light extending in the air outside the fiber. The principle is illustrated in Figure 33. Bringing the fiber close enough to the waveguide to enable good coupling requires very accurate positioning.

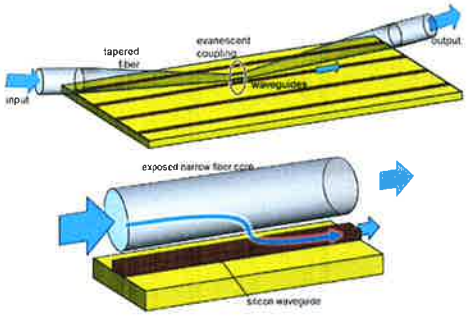

Figure 33: Evanescent coupling between fiber and on-chip waveguides [86].

As with the grating-coupler fiber facets, this technique allows to probe everywhere on the chip. Even better, it is not required to have a broad waveguide section: a narrow wire will do. The evanescent coupling is also used a lot to probe high-quality cavities directly: this way, there is no need to design access waveguides, which generally reduce the quality factor of the cavity.

4.7.3 *Mirrors and cantilevers*

More exotic approaches to coupler light through the chip surface include the use of mirrors (either metal or by total internal reflection). However, because of the small core size of silicon waveguides, this technique is not very efficient. It has been used with larger, lower-contrast waveguides [87].

Another alternative is to bend the on-chip waveguide away from the chip surface. This can be done using techniques from MEMS fabrication, and by tuning the stresses in the chip films. This way, a waveguide can become a pre-stressed cantilever. Upon release from the buried oxide, the cantilever will bend upward. With proper processing, a vertical coupling can be obtained [88].

4.8 Surface coupling: conclusion

Surface coupling has significant advantages over edge coupling, not the least the potential of wafer-scale testing. Grating couplers are the most commonly used structures to enable surface coupling, and while they have limitations in bandwidth, polarization and footprint, we have discussed different techniques to improve on these weaknesses. Note however that not all these tricks can be arbitrarily combined: It is difficult to combine a 2-D coupler or the 1-D coupler with an overlay with apodization. Also, the bidirectional operation of a 1-D duplexer is difficult to combine with curved grating lines.

Still, for many applications grating couplers are the most promising solution to enable simple and efficient coupling.

5 Free-space Coupling

Up to this point, we have primarily focused on coupling light to and from optical fibers. However, in some applications fiber coupling is not necessary, and this changes the requirements for the coupling significantly. For instance, light from a chip could be coupled to a photodetector or camera, where all the light is collected and there is no requirement for a good overlap with a specific mode. Also, different trade-offs between angular spectrum, bandwidth, coupling efficiency and footprint are possible.

5.1.1 *Free-space edge couplers*

When coupling light to free space, one of the key metrics is the numerical aperture (NA): the angle spread in the far field over which light is emitted or captured. In general, we can consider the NA to be inversely proportional to the coupler area: The smaller the size of the emitting region (either the end facet, or the footprint of the grating coupler), the larger the NA and the wider the angular spectrum of the emitted light. Obviously, this also means that the emission into any specific direction is lower.

Both grating couplers and edge couplers can be used for free-space off-chip coupling. For edge couplers, the requirement of tapering to a fiber-matched mode disappears. It is possible to couple light from a silicon wire facet directly to free space: the submicron core will have a quite large NA, as shown in Figure 34a. Also, some care is needed to avoid reflections at the facet.

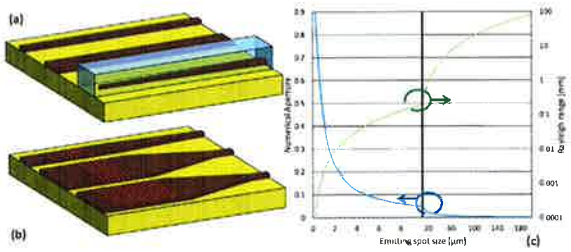

Figure 34: Tuning the numerical aperture for free-space coupling by changing the spot size. (a) edge couplers and (b) grating couplers. (c) The numerical aperture, and its effect on the Rayleigh length, as function of spot size.

5.1.2 *Free-space grating couplers*

Grating couplers can also be used for free-space coupling [89]. The coupler can be made smaller or larger depending on the requirements for numerical aperture. It is also possible to tune the size of the coupler (and thus the numerical aperture) in the two directions individually. This is shown in Figure 34b. In the lateral direction the waveguide can be made narrower, and therefore the NA will become larger in the lateral direction, but the NA in the

longitudinal direction will remain the same. By making the grating teeth stronger, the light will be diffracted more at each tooth, and the exponential decay (shown in Figure 16) will be faster, resulting in a smaller spot radiated upward, and therefore a higher numerical aperture. As the grating coupler is a diffractive structure, it will also increase the bandwidth. Likewise, it is possible to make a narrow-beam, narrow-band coupler by using a very weak grating [90].

As with grating couplers for fibers, it is also possible to make focusing grating couplers for free-space coupling. One can now even change the curved grating lines such that the light is focused above the chip, and the focal distance can be tuned for both x and y separately [91].

5.1.3 Optical Phased Arrays

Up till now we have always considered a single coupling structure for coupling light off-chip. However, we can also employ multiple couplers in a coherent way. By splitting light over several waveguides, one can create an optical phased array. The combined emission pattern of several couplers is then determined by the emission pattern of the individual couplers and their respective phases and amplitudes. In effect, this is a form of multi-path coupling as we have described in paragraph 2.1**Error! Reference source not found.** The principle is illustrated in Figure 35a. The simplest configuration is a periodic array of couplers, with a fixed phase delay between the couplers. In this configuration, the phased array will behave as a much larger grating coupler. A phased array of many small, wide-angle couplers emitting in phase will behave like a much larger, narrow-angle coupler.

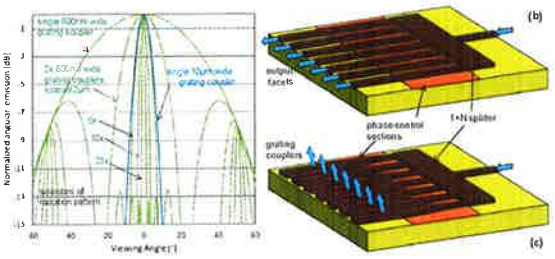

Figure 35: Optical phased arrays. (a) The total emission is a coherent superposition of the emission patterns of the individual couplers. (b) Optical phased array with edge couplers, (c) Optical phased array with grating couplers.

While integrated optical phased arrays have been implemented in AlGaAs [92], silicon photonics could improve the performace through better pattern definition and a smaller footprint.

Optical phased arrays can be implemented with edge coupling and grating couplers. Edge couplers can be organized in a line array, as shown in Figure 35b, while with grating couplers it is even possible to define 2-D phased arrays. The performance of these 2D arrays is still limited due to the low fill factor one can achieve as all the grating couplers need to be accessed with an on-chip waveguide[93]. For a 1D configuration, one does not have this problem and a relatively high fill factor can be obtained.

By changing the phase relation between the couplers many functions are possible. A linear phase shift between subsequent couplers will keep the shape of the narrow beam, but will change the angle of emission. This way, off-chip beam steering is possible [94–98].

By playing with both amplitude and phase, the beam divergence can be tuned from a wide angle to a narrow directed beam. In principle, the emitted phase front can be tuned to a wide extent: the more couplers, the better the control.

By tuning only the phases, a lens can be programmed to focus light on a specific point in space [97]. This is especially useful for sensing applications where light is focused on a spot and the reflection is coupled back into the photonic [99].

Instead of actively tuning the phases using phase tuners, one can also think of using an optical phased array in which the phases are tuned by tuning the wavelength with the use of delay lines. In such a way, one can fabricate a free-space dispersive beam steerer [100] that can find applications in beam steering as well as in demultiplexing [101] and pulse shaping [102].

Because of reciprocity, optical phased arrays can also be used to couple light back onto the chip. This way, a chip can be made to capture light from a tilted or even distorted phase front [103]. The OPA would then act as a coherent receiver allowing phase reconstruction to improve the reception or to perform DOA (Direction Of Arrival) estimation. This can be used in sensing applications where one for example wants to sense light that is reflected from or transmitted through a scattering medium [103].

6 Conclusion

In this chapter, we have tried to give a complete overview of optical coupling solutions between silicon photonic waveguides and optical fibers (and in lesser extent free space). In this we have mainly focused on the on-chip structures, and not gone into detail into packaging solutions. This will be discussed further in this book.

The choice of coupling solution for a particular application will be dependent on the operational specifications, and trade-offs that need to be made between coupling efficiency, bandwidth, footprint and subsequent packaging requirements.

7 Acknowledgements

The authors would like to thank Karel Van Acoleyen, Lars Zimmermann, Zhechao Wang, Sailing He, Yongbo Tang, Attila Mekis, Michael Vanslembrouck, Frederik Van Laere, Shankar Kumar Selvaraja, Kasia Komorowska, Liesbet Van Landschoot, Stijn Scheerlinck Jonathan Schrauwen and Dirk Taillaert for the use of data and illustrations. Part of the results shown here were produced in the framework of the European research project HELIOS. Diedrik Vermeulen thanks the Institute for the Promotion of Innovation by Science and Technology in Flanders (IWT) for a grant.

8 References

[1] R. E. Wagner and W. J. Tomlinson, "Coupling efficiency of optics in single-mode fiber components," *Applied Optics*, vol. 21, no. 15, pp. 2671-2688, 1982.

[2] P. Dumon et al., "Compact wavelength router based on a Silicon-on-insulator arrayed waveguide grating pigtailed to a fiber array.," *Optics express*, vol. 14, no. 2, pp. 664-9, Jan. 2006.

[3] A. Mekis et al., "A Grating-Coupler-Enabled CMOS Photonics Platform," *Selected Topics in Quantum Electronics, IEEE Journal of*, no. 99, pp. 1–12, 2010.

[4] Y. Vlasov and S. McNab, "Losses in single-mode silicon-on-insulator strip waveguides and bends.," *Optics express*, vol. 12, no. 8, pp. 1622-31, Apr. 2004.

[5] I. Day et al., "Tapered silicon waveguides for low insertion-loss highly efficient high-speed electronic variable attenuators," in *Proc. IEEE Opt. Fiber Commun. Conf.*, 2003, pp. 249–251.

[6] T. Tsuchizawa et al., "Microphotonics devices based on silicon microfabrication technology," *IEEE Journal of Selected Topics in Quantum Electronics*, vol. 11, no. 1, pp. 232-240, Jan. 2005.

[7] S. McNab, N. Moll, and Y. Vlasov, "Ultra-low loss photonic integrated circuit with membrane-type photonic crystal waveguides," *Optics express*, vol. 11, no. 22, pp. 2927-39, Nov. 2003.

[8] P. Dumon and R. Baets, "Ultra-Compact Integrated Optical Filters in Silicon-on-insulator by Means of Wafer-Scale Technology," Ghent University, 2007.

[9] V. R. Almeida, R. R. Panepucci, and M. Lipson, "Nanotaper for compact mode conversion," *Optics Letters*, vol. 28, no. 15, pp. 1302-1304, 2003.

[10] T. Shoji, T. Tsuchizawa, T. Watanabe, K. Yamada, and H. Morita, "Low loss mode size converter from 0.3μm square Si waveguides to singlemode fibres," *Electronics Letters*, vol. 38, no. 25, p. 1669, 2002.

[11] L. Chen, C. R. Doerr, Y. K. Chen, and T. Y. Liow, "Low-Loss and Broadband Cantilever Couplers Between Standard Cleaved Fibers and High-Index-Contrast Si3N4 or Si Waveguides," *Photonics Technology Letters, IEEE*, vol. 22, no. 23, pp. 1744–1746, 2010.

[12] M. Pu, L. Liu, H. Ou, K. Yvind, and J. M. Hvam, "Ultra-low-loss inverted taper coupler for silicon-on-insulator ridge waveguide," *Optics Communications*, vol. 283, no. 19, pp. 3678-3682, Oct. 2010.

[13] R. Winn, "No Title," *IEEE Trans. Microwave Theory and Tech.*, vol. 23, pp. 92-123, 1975.

[14] K. Kasaya, O. Mitomi, M. Naganuma, Y. Kondo, and Y. Noguchi, "A simple laterally tapered waveguide for low-loss coupling to single-mode fibers," *IEEE Photonics Technology Letters*, vol. 5, no. 3, pp. 345-347, Mar. 1993.

[15] K. Van Acoleyen and R. Baets, "Compact lens-assisted focusing tapers fabricated on silicon-on-insulator," in *8th IEEE International Conference on Group IV Photonics*, 2011, pp. 157-159.

[16] B. Luyssaert, "Compact Planar Waveguide Spot-Size Converters in Silicon-on-Insulator," Ghent University, 2005.

[17] M. M. Spuhler, B. J. Offrein, G.-L. Bona, R. Germann, I. Massarek, and D. Erni, "A very short planar silica spot-size converter using a nonperiodic segmented waveguide," *Lightwave Technology, Journal of*, vol. 16, no. 9, pp. 1680–1685, 1998.

[18] L. Zimmermann, T. Tekin, H. Schroeder, P. Dumon, and W. Bogaerts, "How to bring nanophotonics to application-silicon photonics packaging," *IEEE LEOS NEWSLETTER*, vol. 22, no. December, pp. 4–14, 2008.

[19] J. Galan et al., "CMOS compatible silicon etched V-grooves integrated with a SOI fiber coupling technique for enhancing fiber-to-chip alignment," in *Group IV Photonics, 2009. GFP '09. 6th IEEE International Conference on*, 2009, no. c, pp. 148–150.

[20] M. R. Watts, H. A. Haus, and E. P. Ippen, "Integrated mode-evolution-based polarization splitter," *Optics Letters*, vol. 30, no. 9, pp. 967-969, 2005.

[21] T. Barwicz et al., "Polarization-transparent microphotonic devices in the strong confinement limit," *Nature Photonics*, vol. 1, no. 1, pp. 57-60, Jan. 2007.

[22] H. Fukuda, K. Yamada, T. Tsuchizawa, T. Watanabe, H. Shinojima, and S.-I. Itabashi, "Ultrasmall polarization splitter based on silicon wire waveguides.," *Optics express*, vol. 14, no. 25, pp. 12401-8, Dec. 2006.

[23] C. R. Doerr and L. Chen, "Monolithic PDM-DQPSK receiver in silicon," in *Optical Communication (ECOC), 2010 36th European Conference and Exhibition on*, 2010, pp. 1–3.

[24] M. R. Watts and H. A. Haus, "Integrated mode-evolution-based polarization rotators," *Optics Letters*, vol. 30, no. 2, pp. 138-140, 2005.

[25] J. Zhang, M. Yu, G.-qiang P. Lo, D.-lee Kwong, and A. A. "Silicon-Waveguide-Based Mode Evolution Polarization Rotator," *IEEE Journal of Selected Topics in Quantum Electronics*, vol. 16, no. 1, pp. 53-60, 2010.

[26] L. Chen, C. R. Doerr, and Y.-K. Chen, "Compact polarization rotator on silicon for polarization-diversified circuits," *Optics letters*, vol. 36, no. 4, pp. 469-71, Feb. 2011.

[27] D. Vermeulen, S. Selvaraja, P. Verheyen, W. Bogaerts, D. V. Thourhout, and G. Roelkens, "High Efficiency Broadband Polarization Rotator on Silicon-On-Insulator," in *Group IV Photonics*, 2010, pp. 42-44.

[28] H. Fukuda, K. Yamada, T. Tsuchizawa, T. Watanabe, H. Shinojima, and S.-ichi Itabashi, "Silicon photonic circuit with polarization diversity," *Quantum Electron*, vol. 16, no. 7, pp. 4872-4880, 2008.

[29] Z. Wang and D. Dai, "Ultrasmall Si-nanowire-based polarization rotator," *Journal of the Optical Society of America B*, vol. 25, no. 5, p. 747, Apr. 2008.

[30] D. Taillaert, P. Bienstman, and R. Baets, "Compact efficient broadband grating coupler for silicon-on-insulator waveguides," *Optics letters*, vol. 29, no. 23, pp. 2749-51, Dec. 2004.

[31] D. Taillaert et al., "Grating Couplers for Coupling between Optical Fibers and Nanophotonic Waveguides," *Japanese Journal of Applied Physics*, vol. 45, no. 8, pp. 6071-6077, Aug. 2006.

[32] A. Mekis et al., "A Grating-Coupler-Enabled CMOS Photonics Platform," *Selected Topics in Quantum Electronics, IEEE Journal of*, no. 99, pp. 1–12, 2010.

[33] S. Scheerlinck, J. Schrauwen, F. Van Laere, D. Taillaert, D. Van Thourhout, and R. Baets, "Efficient, broadband and compact metal grating couplers for silicon-on-insulator waveguides," *Optics express*, vol. 15, no. 15, pp. 9625-30, Jul. 2007.

[34] R. Halir, P. Cheben, S. Janz, D.-xia Xu, I. Molina-fernández, and J. G. Wangüemert-pérez, "Waveguide grating coupler with subwavelength microstructures," *Optics Letters*, vol. 34, no. 9, pp. 1408-1410, 2009.

[35] H. K. Tsang, "Nanoholes Grating Couplers for Coupling Between Silicon-on-Insulator Waveguides and Optical Fibers," *IEEE Photonics Journal*, vol. 1, no. 3, pp. 184-190, Sep. 2009.

[36] L. Liu, M. Pu, K. Yvind, and J. M. Hvam, "High-efficiency, large-bandwidth silicon-on-insulator grating coupler based on a fully-etched photonic crystal structure," *Applied Physics Letters*, vol. 96, no. 5, p. 051126, 2010.

[37] R. Halir et al., "Continuously apodized fiber-to-chip surface grating coupler with refractive index engineered subwavelength structure," *Optics letters*, vol. 35, no. 19, pp. 3243-5, Oct. 2010.

[38] X. Chen and H. K. Tsang, "Polarization-Independent Grating Couplers for Silicon-on-Insulator Nanophotonic Waveguides," *OPTICS LETTERS*, vol. 36, no. 6, pp. 796-798, 2011.

[39] W. Bogaerts et al., "Basic structures for photonic integrated circuits in Silicon-on-insulator," *Optics express*, vol. 12, no. 8, pp. 1583-91, Apr. 2004.

[40] Z. Yu et al., "High efficiency and broad bandwidth grating coupler between nanophotonic waveguide and fibre," *Chinese Physics B*, vol. 19, no. 1, p. 014219-5, Jan. 2010.

[41] J. Bolten et al., "CMOS compatible cost-efficient fabrication of SOI grating couplers," *Microelectronic Engineering*, vol. 86, no. 4-6, pp. 1114-1116, Apr. 2009.

[42] L. Vivien et al., "Light injection in SOI microwaveguides using high-efficiency grating couplers," *Journal of Lightwave Technology*, vol. 24, no. 10, pp. 3810-3815, Oct. 2006.

[43] K. A. Bates, L. Li, R. L. Roncone, and J. J. Burke, "Gaussian beams from variable groove depth grating couplers in planar waveguides," *Applied optics*, vol. 32, no. 12, pp. 2112–2116, 1993.

[44] D. Taillaert, "Grating couplers as Interface between Optical Fibres and NanophotonicWaveguides," Ghent University, 2005.

[45] S. K. Selvaraja et al., "Highly efficient grating coupler between optical fiber and silicon photonic circuit," in *Lasers and Electro-Optics, 2009 and 2009 Conference on Quantum electronics and Laser Science Conference. CLEO QELS 2009. Conference on*, 2009, vol. 1, pp. 1–2.

[46] Z. Wang, Y. Tang, L. Wosinski, and S. He, "Experimental Demonstration of a High Efficiency Polarization Splitter based on a One-Dimensional Grating with a Bragg Reflector underneath," *Photonics Technology Letters, IEEE*, vol. 22, no. 21, pp. 1568-1570, 2010.

[47] F. Van Laere et al., "Compact and Highly Efficient Grating Couplers Between Optical Fiber and Nanophotonic Waveguides," *Journal of Lightwave Technology*, vol. 25, no. 1, pp. 151-156, Jan. 2007.

[48] S. K. Selvaraja et al., "Low-loss amorphous silicon-on-insulator technology for photonic integrated circuitry," *Optics Communications*, vol. 282, no. 9, pp. 1767-1770, May 2009.

[49] C. Kopp, E. Augendre, R. Orobtchouk, O. Lemonnier, and J.-marc Fedeli, "Enhanced Fiber Grating Coupler Integrated by Wafer-to-Wafer Bonding," *Journal of Lightwave Technology*, vol. 29, no. 12, pp. 1847-1851, Jun. 2011.

[50] G. Roelkens, D. V. Thourhout, and R. Baets, "High efficiency grating coupler between silicon-on-insulator waveguides and perfectly vertical optical fibers," *Optics letters*, vol. 32, no. 11, pp. 1495–1497, 2007.

[51] J. W. Goodman, *Introduction to Fourier Optics*, 2nd ed. New York: McGraw-Hill, 1996.

[52] A. Martínez, M. D. M. Sánchez-López, and I. Moreno, "Phasor analysis of binary diffraction gratings with different fill factors," *European Journal of Physics*, vol. 28, no. 5, pp. 805-816, Sep. 2007.

[53] D. Vermeulen et al., "High-efficiency fiber-to-chip grating couplers realized using an advanced CMOS-compatible silicon-on-insulator platform," *Optics express*, vol. 18, no. 17, pp. 18278-83, Aug. 2010.

[54] G. Roelkens et al., "High efficiency diffractive grating couplers for interfacing a single mode optical fiber with a nanophotonic silicon-on-insulator waveguide circuit," *Applied Physics Letters*, vol. 92, no. 13, p. 131101, 2008.

[55] G. Roelkens, D. Van Thourhout, and R. Baets, "High efficiency Silicon-on-Insulator grating coupler based on a poly-Silicon overlay," *Optics express*, vol. 14, no. 24, pp. 11622-30, Nov. 2006.

[56] D. Vermeulen, S. Selvaraja, P. Verheyen, G. Lepage, W. Bogaerts, and G. Roelkens, "High-efficiency silicon-on-insulator fiber-to-chip grating couplers using a silicon overlay," in *Group IV Photonics*, 2009.

[57] T. Saha and W. Zhou, "High efficiency diffractive grating coupler based on transferred silicon nanomembrane overlay on photonic waveguide," *Journal of Physics D: Applied Physics*, vol. 42, 2009.

[58] N. Na et al., "Efficient broadband silicon-on-insulator grating coupler with low backreflection," *Optics letters*, vol. 36, no. 11, pp. 2101–2103, 2011.

[59] C. Alonso-Ramos, A. Ortega-Moñux, I. Molina-Fernández, P. Cheben, L. Zavargo-Peche, and R. Halir, "Efficient fiber-to-chip grating coupler for micrometric SOI rib waveguides," *Optics Express*, vol. 18, no. 14, p. 15189, Jul. 2010.

[60] Y. Tang, Z. Wang, U. Westergren, and L. Wosinski, "High efficiency nonuniform grating coupler by utilizing the lag effect in the dry etching process," in *Optical Fiber Communication Conference*, 2010, pp. 1-3.

[61] X. Chen, C. Li, C. K. Y. Fung, S. M. G. Lo, and H. K. Tsang, "Apodized waveguide grating couplers for efficient coupling to optical fibers," *Photonics Technology Letters, IEEE*, vol. 22, no. 15, pp. 1156–1158, Aug. 2010.

[62] M. Antelius, K. B. Gylfason, and H. Sohlström, "An apodized SOI waveguide-to-fiber surface grating coupler for single lithography silicon photonics," *Optics express*, vol. 19, no. 4, pp. 3592-8, Feb. 2011.

[63] X. Chen, C. Li, H. K. Tsang, and S. Member, "Fabrication-Tolerant Waveguide Chirped Grating Coupler for Coupling to a Perfectly Vertical Optical Fiber," *IEEE Photonics Technology Letters*, vol. 20, no. 23, pp. 1914-1916, Dec. 2008.

[64] J. Schrauwen, F. Van Laere, D. Van Thourhout, and R. Baets, "Focused-Ion-Beam Fabrication of Slanted Grating Couplers in Silicon-on-Insulator Waveguides," *IEEE Photonics Technology Letters*, vol. 19, no. 11, pp. 816-818, Jun. 2007.

[65] J. Schrauwen, S. Scheerlinck, D. Van Thourhout, and R. Baets, "Polymer wedge for perfectly vertical light coupling to silicon," *Proceedings of SPIE*, vol. 32, no. 0, p. 72180B-72180B-8, 2009.

[66] S. Scheerlinck, J. Schrauwen, G. Roelkens, D. Van Thourhout, and R. Baets, "Vertical fiber-to-waveguide coupling using adapted fibers with an angled facet fabricated by a simple molding technique," *Applied optics*, vol. 47, no. 18, pp. 3241-5, Jun. 2008.

[67] D. Vermeulen et al., "Efficient Tapering to the Fundamental Quasi-TM Mode in Asymmetrical Waveguides," in *European Conference on Integrated Optics*, 2010.

[68] D. Taillaert, P. I. Borel, L. H. Frandsen, R. M. De La Rue, and R. Baets, "A compact two-dimensional grating coupler used as a polarization splitter," *IEEE Photonics Technology Letters*, vol. 15, no. 9, pp. 1249-1251, Sep. 2003.

[69] W. Bogaerts, D. Taillaert, P. Dumon, D. Van Thourhout, R. Baets, and E. Pluk, "A polarization-diversity wavelength duplexer circuit in silicon-on-insulator photonic wires," *Optics express*, vol. 15, no. 4, pp. 1567-78, Feb. 2007.

[70] R. Halir, D. Vermeulen, and G. Roelkens, "Reducing Polarization-Dependent Loss of Silicon-on-Insulator Fiber to Chip Grating Couplers," *IEEE Photonics Technology Letters*, vol. 22, no. 6, pp. 389-391, Mar. 2010.

[71] F. Van Laere et al., "Efficient Polarization Diversity Grating Couplers in Bonded InP-Membrane," *IEEE Photonics Technology Letters*, vol. 20, no. 4, pp. 318-320, Feb. 2008.

[72] C. R. Doerr et al., "Monolithic Polarization and Phase Diversity Coherent Receiver in Silicon," *Journal of Lightwave Technology*, vol. 28, no. 4, pp. 520-525, Feb. 2010.

[73] C. R. Doerr, M. S. Rasras, J. S. Weiner, and M. P. Earnshaw, "Diplexer With Integrated Filters and Photodetector in Ge–Si Using <formula formulatype='inline'><tex Notation='TeX'>Γ_{X}</tex> </formula> and <formula formulatype='inline'><tex Notation='TeX'>Γ_{M}</tex> </formula> Directions in a Grating C," *IEEE Photonics Technology Letters*, vol. 21, no. 22, pp. 1698-1700, Nov. 2009.

[74] Z. Wang et al., "Experimental demonstration of an ultracompact polarization beam splitter based on a bidirectional grating coupler," in *Communications and Photonics Conference and Exhibition (ACP)*, 2009, pp. 1-2.

[75] Y. Tang, D. Dai, and S. He, "Proposal for a grating waveguide serving as both a polarization splitter and an efficient coupler for silicon-on-insulator nanophotonic circuits," *Photonics Technology Letters, IEEE*, vol. 21, no. 4, pp. 242–244, 2009.

[76] D. Vermeulen, G. Roelkens, and D. Van Thourhout, "Grating Structures for Simultaneous Coupling to TE and TM Waveguide Modes," 22-Jun-2009.

[77] F. Van Laere et al., "Compact Focusing Grating Couplers for Silicon-on-Insulator Integrated Circuits," *IEEE Photonics Technology Letters*, vol. 19, no. 23, pp. 1919-1921, Dec. 2007.

[78] D. Vermeulen et al., "Reflectionless grating coupling for silicon-on-insulator integrated circuits," in *Group IV Photonics (GFP), 2011 8th IEEE International Conference on*, 2011, vol. 1, no. 1, pp. 74–76.

[79] F. Van Laere, W. Bogaerts, P. Dumon, G. Roelkens, D. Van Thourhout, and R. Baets, "Focusing polarization diversity gratings for Silicon-on-Insulator integrated circuits," in *Group IV Photonics, 2008 5th IEEE International Conference on*, 2008, vol. 1, pp. 203–205.

[80] C. R. Doerr, L. Chen, Y. K. Chen, and L. L. Buhl, "Wide bandwidth silicon nitride grating coupler," *Photonics Technology Letters, IEEE*, vol. 22, no. 19, pp. 1461–1463, 2010.

[81] G. Maire et al., "High efficiency silicon nitride surface grating couplers," *Optics express*, vol. 16, no. 1, pp. 328-33, Jan. 2008.

[82] G. Roelkens, D. Van Thourhout, and R. Baets, "Silicon-on-insulator ultra-compact duplexer based on a diffractive grating structure," *Optics express*, vol. 15, no. 16, pp. 10091-6, Aug. 2007.

[83] D. Vermeulen and G. Roelkens, "Silicon-on-insulator nanophotonic waveguide circuit for fiber-to-the-home transceivers," *2008. ECOC 2008.*, vol. 2, no. September, pp. 1-2, 2008.

[84] S. Scheerlinck, P. Dubruel, P. Bienstman, E. Schacht, D. Van Thourhout, and R. Baets, "Metal Grating Patterning on Fiber Facets by UV-Based Nano Imprint and Transfer Lithography Using Optical Alignment," *Journal of Lightwave Technology*, vol. 27, no. 10, pp. 1415-1420, May 2009.

[85] S. Scheerlinck, D. Taillaert, D. Van Thourhout, and R. Baets, "Flexible metal grating based optical fiber probe for photonic integrated circuits," *Applied Physics Letters*, vol. 92, no. 3, p. 031104, 2008.

[86] C. Grillet et al., "Efficient coupling to chalcogenide glass photonic crystal waveguides via silica optical fiber nanowires," *Optics express*, vol. 14, no. 3, pp. 1070-8, Feb. 2006.

[87] K. Watanabe, J. Schrauwen, A. Leinse, D. V. Thourhout, R. Heideman, and R. Baets, "Total reflection mirrors fabricated on silica waveguides with focused ion beam," *Electronics Letters*, vol. 45, no. 17, p. 883, 2009.

[88] P. Sun and R. M. Reano, "Vertical chip-to-chip coupling between silicon photonic integrated circuits using cantilever couplers," *Optics express*, vol. 19, no. 5, pp. 4722-7, Feb. 2011.

[89] S. a. Masturzo, J. M. Yarrison-Rice, H. E. Jackson, and J. T. Boyd, "Grating Couplers Fabricated by Electron-Beam Lithography for Coupling Free-Space Light Into Nanophotonic Devices," *Nanotechnology, IEEE Transactions on*, vol. 6, no. 6, pp. 622–626, Nov. 2007.

[90] R. Waldhäusl, B. Schnabel, P. Dannberg, E. B. Kley, A. Brauer, and W. Karthe, "Efficient coupling into polymer waveguides by gratings," *Applied optics*, vol. 36, no. 36, pp. 9383-90, Dec. 1997.

[91] J. S. Yang et al., "Novel grating design for out-of-plane coupling with nonuniform duty cycle," *Photonics Technology Letters, IEEE*, vol. 20, no. 9, pp. 730–732, 2008.

[92] F. Vasey, F. Reinhart, R. Houdre, and J. Stauffer, "Spatial optical beam steerin with an AlGaAs integrated phased array," *Applied optics*, vol. 32, no. 18, pp. 3220–3232, 1993.

[93] K. Van Acoleyen, H. Rogier, and R. Baets, "Two-dimensional optical phased array antenna on silicon-on-insulator," *Optics express*, vol. 18, no. 13, pp. 13655-60, Jun. 2010.

[94] A. Hosseini et al., "Unequally Spaced Waveguide Arrays for Silicon Nanomembrane-Based Efficient Large Angle Optical Beam Steering," *Selected Topics in Quantum Electronics, IEEE Journal of*, vol. 15, no. 5, pp. 1439–1446, 2009.

[95] D. N. Kwong, Y. Zhang, A. Hosseini, and R. T. Chen, "Integrated optical phased array based large angle beam steering system fabricated on silicon-on-insulator," *Library*, vol. 7943, no. May, p. 79430Y-79430Y-6, 2011.

[96] K. Van Acoleyen, W. Bogaerts, J. Jágerská, N. Le Thomas, R. Houdré, and R. Baets, "Off-chip beam steering with a one-dimensional optical phased array on silicon-on-insulator," *Optics letters*, vol. 34, no. 9, pp. 1477-9, May 2009.

[97] K. Van Acoleyen, K. Komorowska, W. Bogaerts, and R. Baets, "One-dimensional off-chip beam steering and shaping using optical phased arrays on silicon-on-insulator," *Lightwave Technology, Journal of*, vol. 29, no. 99, pp. 1–1, 2011.

[98] J. K. Doylend, M. J. R. Heck, J. T. Bovington, J. D. Peters, L. a Coldren, and J. E. Bowers, "Two-dimensional free-space beam steering with an optical phased array on silicon-on-insulator," *Optics express*, vol. 19, no. 22, pp. 21595-604, Oct. 2011.

[99] Y. Li, S. Meersman, and R. Baets, "Realization of fiber-based laser Doppler vibrometer with serrodyne frequency shifting," *Applied optics*, vol. 50, no. 17, pp. 2809-14, Jun. 2011.

[100] K. Van Acoleyen, W. Bogaerts, and R. Baets, "Two-Dimensional Dispersive Off-Chip Beam Scanner Fabricated on Silicon-On-Insulator," *IEEE Photonics Technology Letters*, vol. 23, no. 17, pp. 1270-1272, Sep. 2011.

[101] J. Yang, X. Jiang, M. Wang, and Y. Wang, "Two-dimensional wavelength demultiplexing employing multilevel arrayed waveguides," *Optics express*, vol. 12, no. 6, pp. 1084-9, Mar. 2004.

[102] V. R. Supradeepa, C.-B. Huang, D. E. Leaird, and A. M. Weiner, "Femtosecond pulse shaping in two dimensions: towards higher complexity optical waveforms," *Optics express*, vol. 16, no. 16, pp. 11878-87, Aug. 2008.

[103] K. Van Acoleyen, E. M. P. Ryckeboer, K. Komorowska, and R. Baets, "Light collection from scattering media in a silicon photonics integrated circuit," in *IEEE Photonics 2011*, 2011, vol. 4, pp. 543-544.

Series in Optics and Optoelectronics

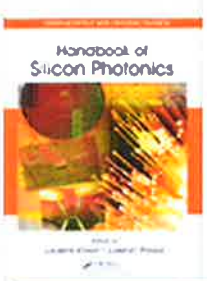

Recommend Title

Handbook of Silicon Photonics

Chapter 3. Off-Chip Coupling

Wim Bogaerts and Diedrik Vermeulen
Citation Information
Handbook of Silicon Photonics
Laurent Vivien and Lorenzo Pavesi
Taylor & Francis 2013
Pages 97–138
Print ISBN: 978-1-4398-3610-1
eBook ISBN: 978-1-4398-3611-8
DOI: 10.1201/b14668-4

3

Off-Chip Coupling

Wim Bogaerts and Diedrik Vermeulen

CONTENTS

Series in Optics and Optoelectronics

About this Book

Recommend Title

Search

Simple Search Advanced Search

All books
This series
This book

Search

Handbook of Silicon Photonics

Citation Information
Handbook of Silicon Photonics
Laurent Vivien and Lorenzo Pavesi
Taylor & Francis 2013
Print ISBN: 978-1-4398-3610-1
eBook ISBN: 978-1-4398-3611-8